J Ther Eng, Vol. 12, No. 2, pp. 550−578, March, 2026

Journal of Thermal Engineering
Web page info: https://jten.yildiz.edu.tr
DOI: 10.14744/thermal.0001101

Research Article

Experimental analysis and optimization of the air-cooled solar panel

Vineet SINGH[1,*], Vinod Singh YADAV[2], Niraj KUMAR[3], Anurag MAHESWARI[4], Javed Khan BHUTTO[5], Sultan ALSHEHERY[6], Mohammed Azam ALI[6], Manoj KUMAR[1]

[1]Department of Mechanical Engineering, School of Engineering & Technology, IFTM University, Moradabad, 244102, India
[2]Department of Mechanical Engineering, NIT, Srinagar Pauri Garhwal, Uttarakhand, 246174, India
[3]Department of Mechanical Engineering and Design Institute, Jaypee Institute of Information Technology, Noida, 201309, India
[4]Department of Mechanical Engineering, Government Polytechnic Mawana Khurd, Meerut, Uttar Pradesh, 250401, India
[5]Department of Electrical Engineering, College of Engineering, King Khalid University, Abha, 61421, Saudi Arabia
[6]Department of Mechanical Engineering, King Khalid University, Abha, 61421, Saudi Arabia

ARTICLE INFO

Article history
Received: 21 December 2024
Revised: 07 March 2025
Accepted: 13 March 2025

Keywords:
Exergy; Fins; MINITAB; Optimization; RSM; Solar Panel

ABSTRACT

The efficiency and sustainability of solar panels throughout the day remain significant challenges, primarily due to the temperature rise in solar cell materials during peak sunlight hours, which reduces their efficiency. This study aims to enhance the efficiency of solar panels using an air-cooling mechanism. Based on prior insights, an indoor experimental setup was developed, featuring a cooling system with 196 circular pin fins, each with a diameter of 3 mm and a length of 16 mm, mounted on the rear surface of the solar panel. An aluminum heat sink of 3 mm thickness was integrated to support the fins, while a variable-speed fan supplied airflow across the fins. The solar flux and airflow rate were identified as critical parameters influencing solar panel efficiency. These parameters were optimized using Response Surface Methodology, with ranges of 400–800 W/m² for solar flux and 0.01–0.02 m³/s for airflow rate. Optimization was performed using MINITAB 17 and Design Expert 18 software. The optimized input conditions, solar flux of 403.33 W/m² and airflow rate of 0.0221 m³/s, yielded the following outcomes: exergy efficiency of 15.79%, power output of 4.12 Wp, module temperature of 22.43°C, and solar panel efficiency of 14.48%, with a composite desirability score of 0.5737. This work is novel and new in its simple and light weight arrangement as compared to heavy vibrating pumps required in liquid and nano-fluid cooling. Additionally, the optimization approach and economic analysis of the solar panel cooling system are relatively new and have received little attention in previous literature. Perturbation plots revealed that solar flux had a more pronounced effect on panel performance compared to airflow rate. This study highlights the potential of air-cooling systems to mitigate midday efficiency losses and improve the operational sustainability of solar panels. The findings contribute to advancing cooling technologies for solar energy systems, promoting greater energy efficiency and reliability.

Cite this article as: Singh V, Yadav VS, Kumar N, Maheswari A, Khan Bhutto J, Alshehery S, et al. Experimental analysis and optimization of the air-cooled solar panel. J Ther Eng 2026;12(2):550−578.

***Corresponding author.**
*E-mail address: vineetpsh@gmail.com

This paper was recommended for publication in revised form by Editor-in Chief Ahmet Selim Dalkilic

INTRODUCTION

Environmental problems and economic crises of fossil fuels search the alternative methods for energy production. Solar energy is one of the best ways to convert it into electrical energy. The solar panels show its importance by directly converting solar energy into useful electrical energy. The solar panel is formed by the parallel and series combination of the solar cells. The solar cell is formed by the P-N junction in which holes and electrons cross the depletion layer by absorbing the solar energy. However, the number of factors affect the performance of the solar panel of which some factors are external and internal. The external factors are uncontrollable by the human being but the internal factors can be controlled and modified to hike the solar panel's performance [1]. The higher surface temperature of the solar cell enhanced the thermal resistance of the depletion layer and slowed down the speed of the electrons, so the performance of the PV module was lacking. However, a number of design have been investigated to cool the solar panel, the purpose is to avoid over heating and sustain the performance. A number of cooling methods like active [2, 3, 4], passive [5, 6, 7], nanoparticles [8, 9, 10] and PCM combined with other cooling [11, 12, 13] fluids have been used.

Active cooling requires an external energy source to pump the water and air. The active cooling enhances the heat transfer coefficient and turbulence due to that it has large ability to cool the solar cell. It included the forced air, forced water, and PV/T system. In the active cooling method, the net power produced by the photovoltaic module is obtained by deducting the pump or blower power from the solar panel output power. The passive cooling method requires no additional prime mover; it's based on fully natural circulation. The heat pipe, natural air, and water circulations are considered to be passive cooling approaches in which heat transfer is lower leading to poor performance at higher temperatures. The main advantage of passive cooling is its lower cost due to negligible variable cost. It improved the productivity of solar panel very little due to natural circulation. The Phase Change Material (PCM) works well for performance enhancement of the solar panel by absorbing maximum heat trapped inside it. In the primary heating process, PCM material starts to heat with melting and absorbs a part of sensible heat. In secondary heating, the phase change of PCM material starts which absorbs the latent heat. Due to the heat absorption from the PV cell during day time, the PV cells cooled and produced more power. The cycle is reversed at night time, at the time of the absence of the Sun, which cools down the solar panel, and PCM material reaches in initial state.

PCM cooling gets popularity due to its large absorption capacity, low cost, and chemical stability. The selection of the PCM material depends on the maximum, and minimum temperature of the solar panel and atmospheric temperature. Based on these temperature ranges, the PCM material properties selected, the main PCM material properties are namely thermal, physical, kinetic, chemical, economic, and environmental listed in [14]. Rok et al. [15] performed an experimental and numerical simulation on the performance improvement of the 250 W solar panel using PCM cooling. The RT28HC is used as a PCM material for the cooling of solar panel. The experimental results depicted that PCM material reduced the surface temperature of solar panel by 35.6°C as compared to without cooled solar panel. Rajvikram et al. [16] enhanced the thermal conductance of PCM by using the aluminum sheet as a thermal conductivity enhancer. The test has been conducted for three months. The outcomes of the study indicated that if PCM material with an aluminium sheet attached at the back of the solar panel, the average efficiency enhanced to be 24.4% with an ordinary decline in the temperature of the 10.35°C. Yahya et al. [11] investigated the multi-layered PCM material in solar panel temperature reduction. The approach involves integrating PCM with metallic PCM attached at the back end of the solar panel. The ANSYS FLUENT software has been used for determining the solidification and melting phase. This cooling system enhanced the PV module performance by 35.8% compared to the panel without cooling at the ambient temperature of 40°C and solar flux of 1000 W/m^2.

Fatih et al. (2020) studied the performance of the phase change material, thermoelectric, and aluminium fins on the solar panel cooling. The outcomes of the study saw that the aluminium fins produced the maximum power and the PCM and TEM generated the lowest power. The PCM material worked as the insulator due to the lesser thermal conductivity of the PCM material. Mais et al. [17] experimented to determine the cooling effect of the RT 35 (PCM) on solar panel. The outcomes of the study show that the 16°C temperature has been reduced by using PCM but If the rectangular fins have been used as the thermal conductivity enhancer then further 2°C temperature drop was again achieved. Rajvikram et al. [18] investigated the PCM, fins, and water for the cooling of the solar panel. The outcomes of the study depicted that in two consecutive days reading, the power output enhanced to 8.12% and 9.39% higher than without cooled solar panel. The temperature measurement of the cooled and without cooled solar panel were lower than the 50°C and 70°C.

The thermoelectric cooling, worked on the principle of the Peltier Effect requires no cooling fluids, only electric energy is required to cool the solar panel. In this cooling, a cold and hot heat source has been generated in which heat flow occurs from lower to higher temperatures. The amount of cooling provided by this technique is lower than the active cooling but more than the passive cooling.

The active cooling technique with forced air cooling, required little design change and feasible to fit fan and blower with the solar panel. A number of researchers published the work on active air cooling. In the below section active air cooling on solar panels is given concisely.

Teo et al. [2] explored the effect of air cooling on the power output of the solar panel, and results were compared with those without a cooled solar panel. The results indicated that

the overall temperature reduced by this approach was 30°C, and efficiency improvement recorded to be 4%. Golzari et al. [19] experimentally investigated, the effect of air cooling channel on the performance of the solar panel. The results showed, that solar panel temperature was reduced by 5°C and efficiency improvement of the solar panel was recorded to be 2.6%. Elminshawy et al. [20] performed the experimentation on solar panel cooling by geothermal air cooling. It reduced the solar panel temperature by 9.75°C and improved the solar panel efficiency by 22.98%. Arifin et al. [21] investigated the effect of the aluminum rectangular fin on the heat transfer rate and performance improvement of the solar panel, due to this cooling, the maximum temperature of the solar panel decreased from 85.3°C to 72.8°C. Lebbi et al. [22] investigated the effect of water and air cooling on the back and the front side of the solar panel, for water cooling drip irrigation system was used, and the fan was used for air flow. This cooling effect condensed, the module temperature by 15°C and raised the panel efficiency by 5.7%.

Saleri et al. [23] used thermoelectric cooling on the rear side of the solar panel to lower the solar panel temperature and enhance efficiency. This design has been proven to reduce the solar panel temperature by 15°C and heighten the efficiency by 5.7%. Li et al. [24] investigated the influence of compressed air on the cleaning and cooling of the solar panel. The results reveal that, the efficiency improvement of the solar panel was recorded to be 33.42% by using this technique. Almuwailhi and Zeitoun [25] conducted experiments on solar panel cooling in natural convection, forced convection, and evaporative cooling, and compared the results with those without cooled solar panel. They identified, the temperature of the solar panel lessened by 6°C in forced air cooling with efficiency improvement recorded to be 4% by use of this cooling technique. Abdullah et al. [26] conducted, a study on the air cooling on the efficiency of the solar panel. They identified, the efficiency improvement of the solar panel recorded to be 0.8% as compared to without air-cooled solar panel. Abdullah et al. (2024) [27] investigated experimentally a photovoltaic solar panel on Trombe wall for heating the room in the winter season. This system operates with the help of solar energy without supplying electricity. The experimental models have been prepared, one with DC fan and other without DC fan. The outcomes of the study revealed that the system having the DC fan has higher electrical and thermic efficiency as compared to another system. Abhijeet et al. (2024) [28] performed the energy and exergy analyses of the 380 kW power roof top photovoltaic grid-connected system. They concluded that the system generated the 732.4 kWh/year through this plant. Furthermore, results have been validated with the responses' neural network linear, non-linear, and exponential behaviour. Amjad et al. (2025) [29] used a porous medium to cool the solar panel. They concluded that the solar panel efficiency enhanced to the level of 19% and 5.1% efficiency increased as compared to without cooled solar panel. The cooling fluids properties are responsible for desirable heat transfer and solar panel performance. On the other hand, the various researchers used the number of designs at the rear side of the solar panel. Table 1 presents the various designs of solar panel cooling, used previously so far.

Table 1. Various design of the heat sink with air cooling in solar panel

S. No.	Author,s Description	Design Description	Design Picture	Outcomes of the study
1	Choi et al. [3] (2022)	Dimples were provided on the rear side of the solar panel.	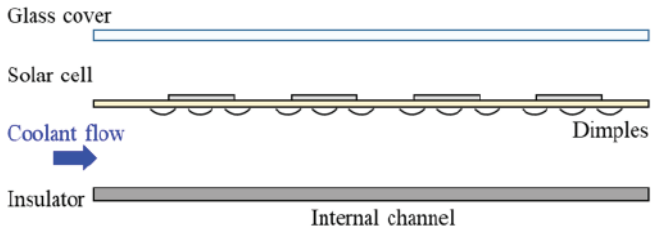	At St =1.1 Heat to mass transfer enhanced by 68%.
2	Hussein et al. (2023)[30]	A cooling air duct was provided at the rear side of the solar panel.		Enhanced the efficiency 2.1% and save, the energy around 7.9%

3	Nabil et al. (2022) [31]	Front side cooling was providing by open air cooling.	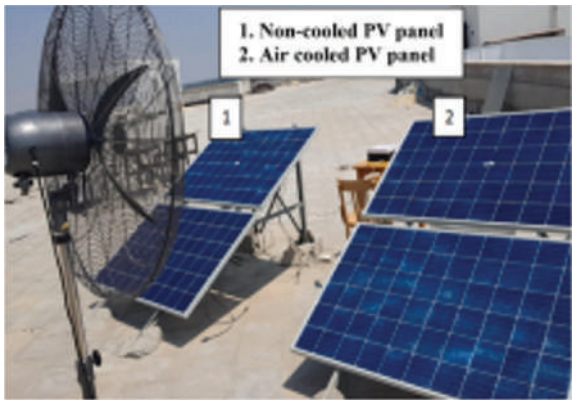	increase the efficiency of solar panel by 2.9%.
4	Amelia R. A. et al. [32]	Used dc fans to blow the dry air.	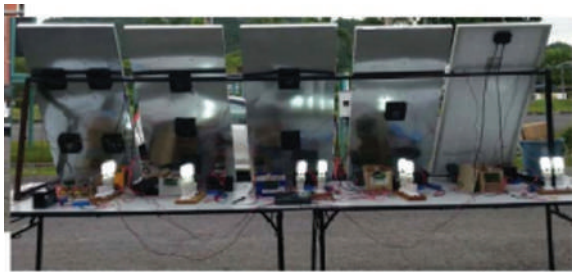	The increasing the number of fans enhanced the power output. If the one fan used then power output increased 12.93%, if the dc fan increased 2, 3 and 4, the power output increased 37.17%, 41.28% and 44.34% respectively.
5	Hernandez et al. (2013) [33]	Create the air channel path at the back of solar panel and used the forced air to cooled.		7.5% power output can be enhanced by use of this technology.
6	Hernandez-Parez et al. (2019) [34]	A heat sink fixed at the back of the solar panel.	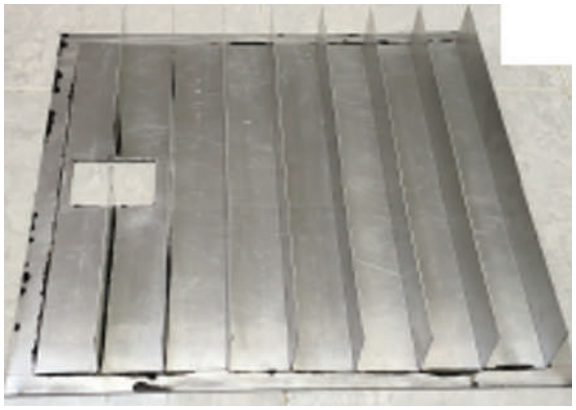	Reduced, the solar panel temperature around 10°C at peak sunny hours.

7	Feng et al. (2018)[35]	Cross fins heat sink fixed at the back side of the solar panel.	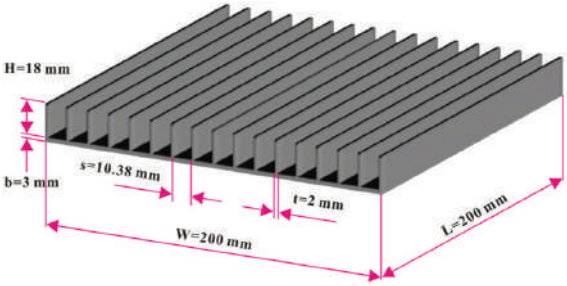	Enhanced, the heat transfer coefficient by 15%.
8	Huang et al. (2014) [36]	A heat sink of long rectangular fin fixed at the bottom side of the solar panel.	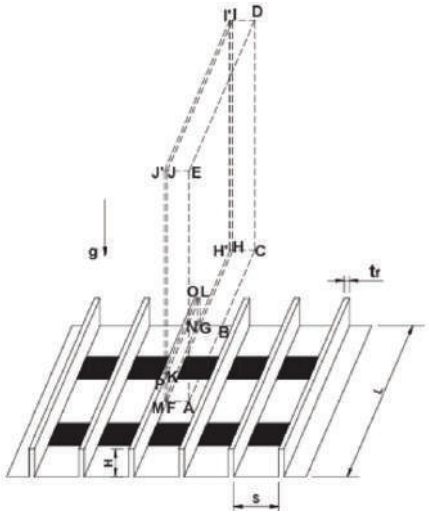	Enhanced performance at due to increased mass flow rate of air.
9	Shaeri et al. (2017) [37]	Long rectangular fins have been attached at the back end of the solar panel.	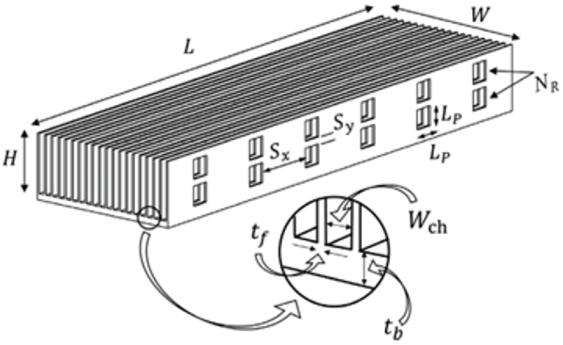	Mass based thermal resistance have been reduced by 49%.
10	Chu et al. (2019) [38]	A heat sink of triangular fins having alternative layout fitted at the back side of the solar panel	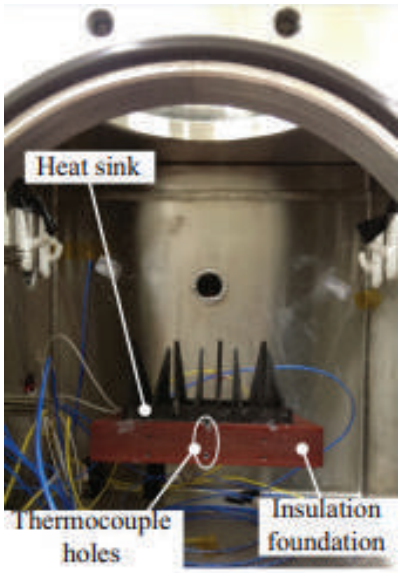	The heat transfer coefficient enhanced by 16%.

Research Gap, Novelty and Application of the Work

Table 1 displays, the several designs of heat sink produced at the rear side of the solar panel in air cooling. The air cooling is feasible requires little change in design at the rear side of the solar panel. Fins are produced on the cooling surface to enhance; the heat transfer by increasing the surface area of the cooling surface. In previous research, rectangular fins were mostly used in the study and very few researchers focused on the high-density pin fins [37]. Although, cylindrical high density pin fins can be produced in large numbers as compared to rectangular fins for making the heat sink compact. Therefore, in this study, high-density pin fins were integrated into the rear surface of a solar panel, and an optimization technique was employed to determine the optimal heat flux and air flow rate for maximizing the panel's performance. The use of high-density pin fins significantly improves the efficiency and operational lifespan of the solar panel. Enhanced efficiency leads to increased power production and a reduction in the panel's size, allowing for the same power output to be achieved at a lower investment cost. This work is novel and new in its simple and light weight arrangement as compared to heavy vibrating pumps required in liquid and nano-fluid cooling. Additionally, the approach of optimization and economic analysis of the solar panel cooling system is also new very little focused in the previous literature with high density pin fins.

The reduced investment cost makes solar panels more accessible and appealing, particularly to farmers and economically disadvantaged communities, encouraging wider adoption to meet energy demands. Furthermore, the lower cost of solar-powered irrigation reduces farming expenses, thereby increasing farmers' profitability. This approach addresses a critical societal challenge by promoting sustainable and cost-effective energy solutions for agriculture and beyond.

EXPERIMENTAL SETUP

Figure 1(a) illustrates the experimental arrangement of the solar panel air-cooling system. The setup consists of two 10 Wp solar panels as presented in Table 2 in which first solar panel is without fins and the second is with fins. The second number of solar panel consists of 196 cylindrical fins, each with an external diameter of 3 mm and fin length of 16 mm. The fins are arranged in horizontal and vertical rows with a spacing of 10 mm and 23 mm, as depicted in Figures 1(b) and 1(c). The solar panel size measures to be 323 mm in length and 217 mm in width. The experimental investigation was conducted to measure various parameters, including solar flux intensity, ambient temperature, photovoltaic (PV) module temperature, air velocity, current, and voltage generated by solar panels. The total experimental observations collected was 13 as per the requirement of Design Expert software for optimization purposes, with the corresponding data summarized in Table 3. These runs provided a comprehensive dataset for analyzing and optimizing the performance of the solar panel cooling system.

Table 2. Specification of solar panels

Parameters	Nominal Value
Nominal Maximum Power (P_m)	10 W
Max voltage (V_m)	18.00 V
Max current (I_m)	0.6 A
Open circuit voltage (V_{OC})	22.00 V
Short circuit current (I_{SC})	0.71 A
Module Efficiency (η_P)	15.4%
Cell Material	Polycrystalline Si
Size	323 mm*217 mm*30 mm
Operating Temperature Range	-40 °C to +80 °C
Temperature Coefficient	-0.2726 %/°C
NOCT	48 °C

Instruments played a critical role in capturing measured data during the experiments. A pyranometer was used to measure solar flux intensity, thermocouples were employed to record surface and air temperatures, an anemometer determined air velocity, and a multimeter was utilized to measure current and voltage outputs from the solar panel. The experiments were conducted at varying discharges of the air (0.01 m^3/s to 0.02 m^3/s) on three consecutive dates in the months 14, 15, and 16 which gives the average reading of the months. The experimental data have been collected from the (01/01/2023 to 21/12/2023). The schematic representation of the experimental setup with instruments is given in Figure 2. Details regarding the accuracy and measurement ranges of the instruments are provided in Table 4.

MODELLING OF THE SOLAR PANEL WITH FINS

Figure 3(a) illustrates the different layers of the solar panel along with the pin fins attached to its rear side. The material properties of each layer are detailed in Figure 3(a) and summarized in Table 5. The solar cell layer exhibits an absorptivity of 1, ensuring no heat flux passes through it; instead, heat transfer occurs from the solar cell to the lower layers of the panel due to the temperature gradient. When solar flux is incident on the panel, the solar cell reaches the highest temperature among all layers, causing heat transfer both to the upper and lower surfaces of the panel.

Figure 3(b) presents the thermal resistance circuit diagram for the solar panel cooling system. Heat transfer from the solar cell occurs primarily through conduction in the top and bottom layers, with the conduction resistances of each layer represented in the diagram. At the top, heat dissipates through a combination of convection and radiation. On the bottom side, heat transfer is improved by the addition of circular pin fins and fan-forced convection. Consequently,

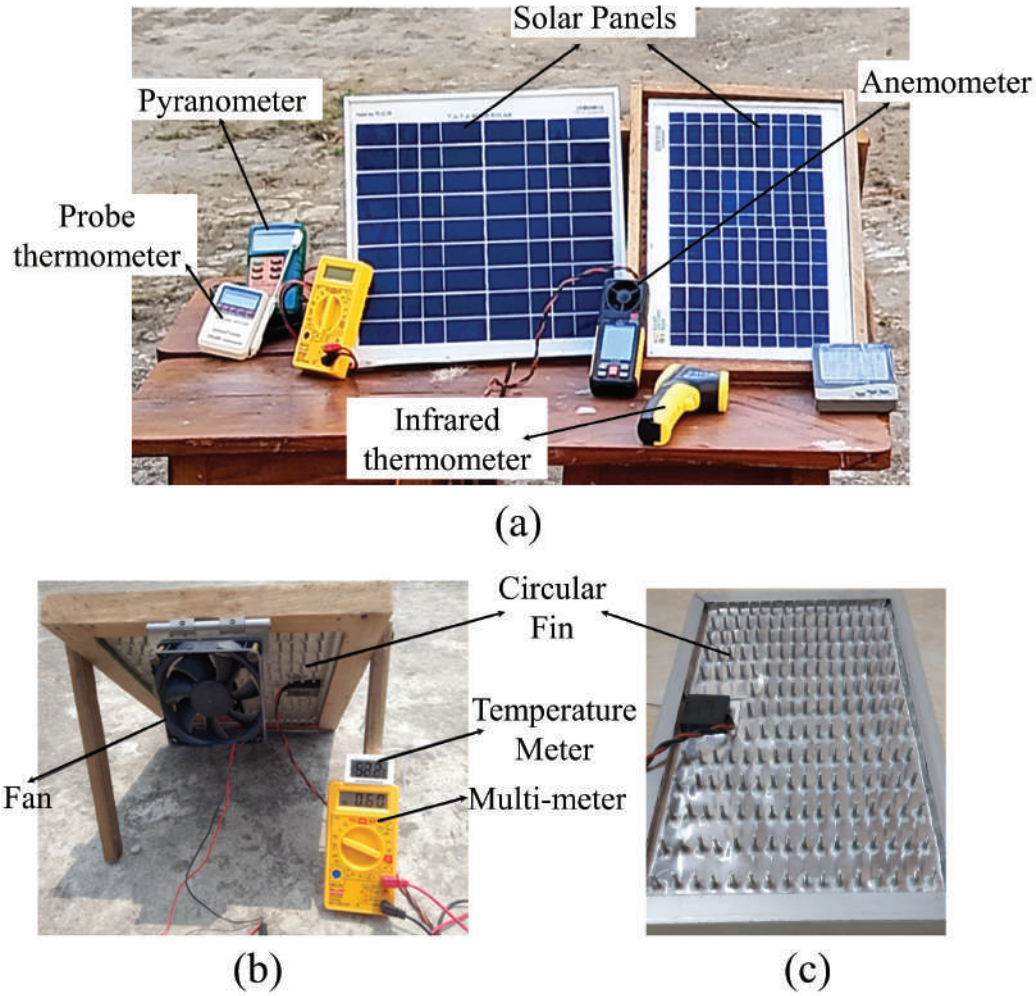

Figure 1. Solar panel air cooling system (a) Experimental setup (b) Rear side of experimental setup (c) Rear side of the solar panel with circular fins.

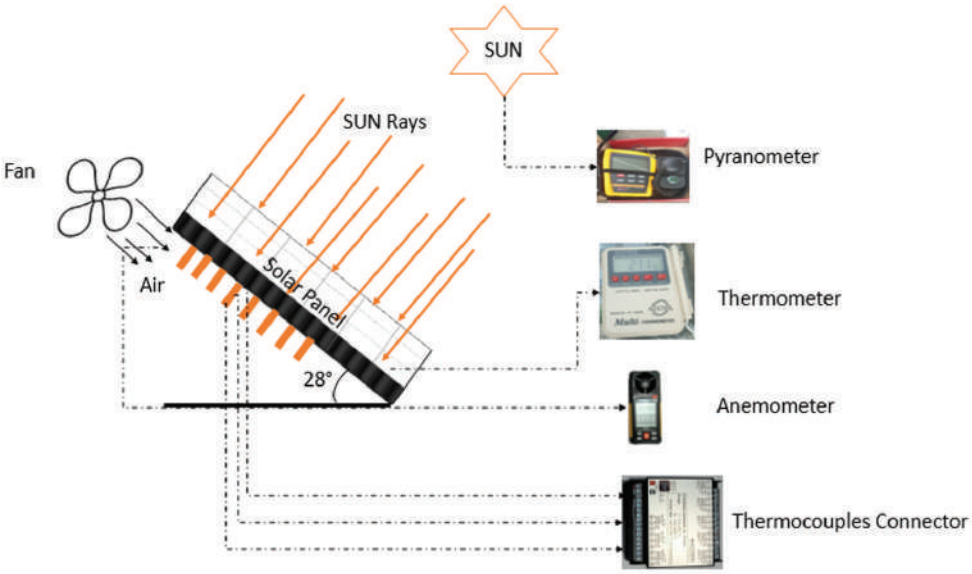

Figure 2. Schematic representation of the Experimental setup.

Table 3. Experimental data of 13 runs of the experimental observations

Run	Solar Flux (W/m^2)	Air Flow Rate (m^3/s)	Module Temperature (°C)	Power Output (W)	Solar Panel Efficiency (%)	Exergy Efficiency (%)
1	400	0.02	23.7432	4.07912	14.3631	15.658
2	600	0.015	49.9903	5.11237	12.0009	13.0828
3	600	0.015	49.9903	5.11237	12.0009	13.0828
4	600	0.015	49.9903	5.11237	12.0009	13.0828
5	600	0.015	49.9903	5.11237	12.0009	13.0828
6	600	0.0220711	47.0408	5.22545	12.2663	13.3722
7	600	0.015	49.9903	5.11237	12.0009	13.0828
8	800	0.02	62.8051	6.1614	10.8475	11.8255
9	400	0.01	28.6053	3.95485	13.9255	15.181
10	800	0.01	66.4771	5.97369	10.5171	11.4652
11	317.157	0.015	10.7076	3.49849	15.5363	16.937
12	600	0.00792893	52.8758	5.00174	11.7412	12.7997
13	882.843	0.015	69.2981	6.43314	10.2632	11.1885

Table 4. Performance parameters of the measuring instruments

Instrument	Model	Range	Accuracy
Temperature measurement	J K PT-100, 8 channel scanner	J: 0-600°C K:0-1200°C	4.25%
Velocity measurement	AVM-03 Digital Anemometer	0-30 m/s	4%
Solar Flux Intensity	LX -107 Solar Power Meter	Lux: 2000 W/m^2	5%
Surface contact temperature measurement	ST-92838 Multi Thermometer	-50 to 300°C	3.5%

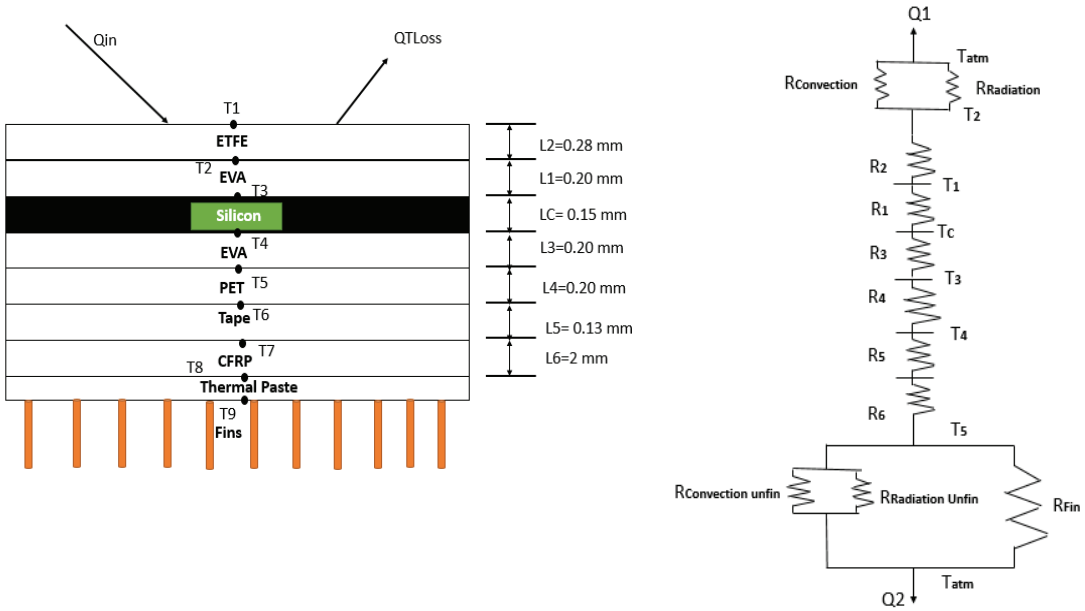

(a) Layers of the solar panel and the fins

(b) Resistance diagram of the heat transfer in solar panel

Figure 3. Heat transfer layers and resistance network.

the bottom layer dissipates heat to the atmosphere through the fins and the un-finned areas of the panel›s rear surface.

The total amount of heat transfers from solar cells to the atmosphere.

$$Q_{Cell} = Q_1 + Q_2 \quad (1)$$

Q_{Cell} is the heat flow through the solar cell, Q_1 is the heat flow through the top surface of the solar panel, Q_2 is the heat flow through the bottom surface of the solar panel.

$$Q_{cell} = \frac{T_C - T_{atm}}{R_1 + R_2 + \frac{R_{Convection} R_{Radiation}}{(R_{Radiation} + R_{Convection})}} + \frac{T_C - T_{atm}}{R_3 + R_4 + R_5 + R_6 + \frac{R_{Unfin} R_{Fin}}{R_{unfin} + R_{Fin}}} \quad (2)$$

Where T_C is the cell temperature, T_{atm} is the atmospheric temperature, R_1, R_2, R_3, R_4, R_5 and R_6 are the thermal resistance of the conduction of various layers of the solar panel, $R_{Convection}$ is the convection resistance from top surface, $R_{Radiation}$ is the radiation resistance from the top surface, R_{Fin} is the thermal resistance due to fins, R_{Unfin} is the thermal resistance due to unfin surface area.

The unfin rear side surface of the solar panel contributes the heat transfer by convection and radiation.

So the thermal resistance of the unfin surface of the PV modules is assumed by the following relation.

$$R_{unfin} = \frac{R_{Convection\ unfin} R_{Radiation\ Unfin}}{R_{Convection\ Unfin} + R_{Radiation\ Unfin}} \quad (3)$$

Where $R_{Convection\ unfin}$ is the unfin surface convection resistance and $R_{Radiation\ Unfin}$ is the unfin surface radiation thermal resistance.

The R_1, R_2, R_3, R_4, R_5 and R_6 are thermal resistance of the conduction of various layers of the solar panel. The values of these thermal are given below.

$$R_1 = \frac{L_1}{K_1 A},\ R_2 = \frac{L_2}{K_2 A},\ R_3 = \frac{L_3}{K_3 A},\ R_4 = \frac{L_4}{K_4 A},$$
$$R_5 = \frac{L_5}{K_5 A},\ R_6 = \frac{L_6}{K_6 A}$$

Where L_1, L_2, L_3, L_4, L_5, and L_6 are the thickness of the several covers of the solar panel presented in Figure 3 (a). K_1, K_2, K_3, K_4, K_5 and K_6 are the thermal conductivity of the EVA, ATFE, EVA, PET, TAPE, and CFRP layers of the solar panel, A is the surface area of the solar panel.

The convection and radiation thermal resistance of the top surface of the solar panel of material ETFE is given by the following equations.

$$R_{Convection} = \frac{1}{h_C A} \quad (4)$$

Where h_C is the solar panel top surface convection heat transfer coefficient.

$$R_{Radiation} = \frac{1}{\sigma \varepsilon A (T_C + T_{atm})(T_C^2 + T_{atm}^2)} \quad (5)$$

Where σ is the Stefan Boltzmann Constant and ε is the emissivity of the upper layer of the solar panel.

The unfin surface convection and radiation thermal resistance also represented by following equations [39].

$$R_{Convection} = \frac{1}{h_{Cb} A_{Unfin}} \quad (6)$$

Where h_{Cb} is the convection heat transfer coefficient from unfin surface and A_{Unfin} is the unfin surface area of the solar panel.

$$R_{Radiation} = \frac{1}{\sigma \varepsilon A_{Unfin} (T_{Cb} + T_{atm})(T_{Cb}^2 + T_{atm}^2)} \quad (7)$$

Where T_{Cb} is the temperature of the base of the solar panel.

The fin thermal resistance for the convection boundary is represented by the following equation.

$$R_{Fin} = \frac{TC_b - T_{atm}}{q_{Fin}} \quad (8)$$

Where q_{Fin} is the heat flow through the fins.

$$R_{Fin} = \left[1 + \frac{mL\emptyset}{Bi_C}\right]\left[\sqrt{hpkA}\emptyset\right]^{-1} \quad (9)$$

Where m is the constant depending on the fin length and diameter and L is the length of the fins.

Where φ is the function represented by the following equation [40].

$$\emptyset = \frac{mLtanhmL + Bi_e}{mL + Bi_e tanhmL} \quad (10)$$

Where B_{ie} is the fin tip Biot Number, B_{ic} is the fin base Biot Number and B_i is the fin Biot Number.

$$B_{ic} = \frac{h_c L}{k}, B_{ie} = \frac{h_e L}{k}, B_i = \frac{h t_e}{k} \quad (11)$$

Where L is the length of the fin, k is the thermal conductivity of the fin material represented in Table 4, t_e is the fin tip thickness, A is the crossectional area of the fin base and p is the perimeter of the fin tip.

The h_c is the fin base contact conductance for aluminium it is taken as 1000 W/m^2. k, h is the fin convection coefficient and h_e is the fin tip convection coefficient.

The h and h_e is found by the following formula of the Nusselt Number [41].

$$Nu = \left[\frac{1}{\frac{(RePr)^3}{8}} + \frac{1}{\left[0.664\left(\sqrt{Re}\right)(Pr^{0.33})\left(\sqrt{(1} + \frac{3.65}{\sqrt{Re}}\right)\right]^3}\right] \quad (12)$$

Where R_e and P_r is the Reynold Number and Prandlt Number of the air.

The Pr is the Prandlt Number calculated by following the formula [42].

$$Pr = \frac{\mu C_P}{k}, Re = \frac{\rho V D_h}{\mu} \quad (13)$$

Now heat transfer coefficient has been determined by the subsequent equation [43].

$$h = h_e = \frac{Nuk}{D_h} \quad (14)$$

where ρ, μ, and k are the density, dynamic viscosity, and thermal conductivity of the air. The D_h represents the hydraulic diameter of the pin fin.

Efficiency and Exergy of the Solar Panel

Figure 4 represents the various energy interactions in the control volume of the solar panel. The W_p represents the pump work, W_e is the solar panel electrical work, Q_{in} is the solar energy reached on the solar panel, Q_{out} is the energy lost in the atmosphere, and CV is the control volume. The system is considered to be a steady state with kinetic and potential energy terms of the air at the inlet and outlet are neglected. To apply the first law of thermodynamics for the Figure 4 control volume [44].

$$\frac{dU_{CV}}{dt} = (Q_{in} - Q_{out}) - (W_e - W_p) + m_{air}(h_1 - h_2) \quad (15)$$

Where h_1 and h_2 are the enthalpy of the air at the inlet and outlet section of the solar panel. m_{air} is the mass flow rate of the air.

$$\text{At steady state, } \frac{dU_{CV}}{dt} = 0 \quad (16)$$

$$0 = Q_{in} - Q_{out} - W_e + W_p + m_{air}C_p(T_1 - T_2) \quad (17)$$

$$Q_{in} + W_p = W_e + m_{air}C_p(T_2 - T_1) + Q_{out} \quad (18)$$

In equation (18), the left-hand part represents the input energy, and right-hand side first part represents the electric work output, the second part represents the heat carried by air and the third part represents the energy loss in the atmosphere.

The electrical efficiency of the solar plate is given by the following relation

$$\eta_e = \frac{W_e}{Q_{in} + W_p} \quad (19)$$

η_e is the effective efficiency of the solar panel.

Now apply the exergy balance for the solar panel control volume [45]

$$\frac{dE_{XCV}}{dt} = E_{Xin} - E_{Xout} - E_d \quad (20)$$

Where E_{Xin} is the exergy entering the PV module, E_{Xout} called the exergy leaving the system, E_d is the exergy destruction inside the system.

$$\text{For steady state } \frac{dE_{XCV}}{dt} = 0 \quad (21)$$

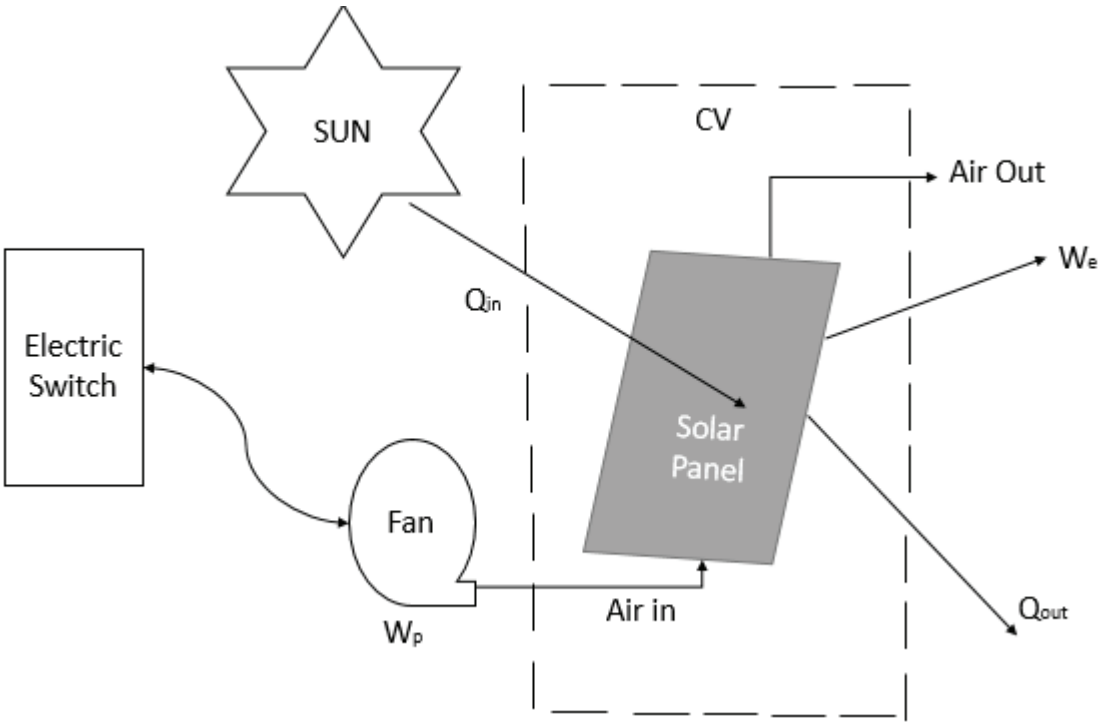

Figure 4. Heat and Work Interactions within the Solar Panel's Control Volume.

$$E_{Xin} = E_{Xout} + E_d \quad (22)$$

$$E_{SUN}+W_p+m_{air}\varphi_1=\left(1-\frac{T_{atm}}{T_b}\right)Q_{out}+W_e+m_{air}\varphi_2+E_d \quad (23)$$

Where E_{SUN} is the exergy received from the Sun and φ1 and φ2 are the inlet and outlet flow exergy.

$$E_{SUN}+W_p=W_e+m_{air}(\varphi_2-\varphi_1)+\left(1-\frac{T_{atm}}{T_b}\right)Q_{out} \quad (24)$$

Equation (22) left hand term represents the exergy supplied to the solar panel, right hand side first term represents the exergy recovered, second term shows the exergy recovered by air and third term represents the exergy loss in the atmosphere.

Now exergetic efficiency of the air

$$\varphi = \frac{W_e}{E_{SUN}+W_p} \quad (25)$$

The exergy reached on the solar panel [46].

$$E_{SUN} = A_P I_t[1 - \frac{4}{3}\left(\frac{T_a}{T_{SUN}}\right) + \frac{1}{3}\left(\frac{T_a}{T_{SUN}}\right)^4] \quad (26)$$

Cost Estimation of the Solar Panel

The cost estimation of the modified solar panel justifies the suggested cooling techniques. The best way to compare the Levelized Cost of Energy (LCOE) of the simple solar panel and the modified solar panel. The LCOE is the ratio of the total investment in the life cycle of the solar panel to the total power production by the solar panel in its life cycle. The total investment of the project is the sum of the cost of the solar panel, material cost, manufacturing cost, maintenance, operational cost, and fixed cost. The total power production is counted in kWh with every year depreciation will be counted. So following equation has been used for the calculation of the LCOE of the system.

$$LCOE = \frac{\sum_0^n \frac{(I+M+F)}{(1+r)^n}}{\sum_0^n (\frac{E}{(1+r)^n}} \quad (27)$$

Where I is the investment, M is the maintenance cost, F is fixed cost and E is energy produced throughout the life cycle, r is the discount rate and n is the number of years.

The initial investment is the sum of the cost of the solar panel, material, and manufacturing. It is assumed by the following relation.

$$I = xp + \rho vy + m \quad (28)$$

Where x is the cost of the solar panel ($/Wp), p is the power of the solar panel, ρ is the density of fin materials, v is the volume of the fins material, y is the cost of the material ($/kg), m is the manufacturing cost. The volume of the fins is given by the following equation.

$$v = \frac{\pi}{4} d^2 L \quad (29)$$

Where d is the diameter and L is the length of the fins.

Optimization Technique

The optimization has been performed to know the optimum values of the input variables on which, the system of the solar panel cooling gives the maximum power output and efficiency. For which Response Surface Methodology (RSM) has been used. In year 1951 [47], RSM was used in chemical industries for improving production but recent times due to development of the various Design of Experiment (DoE) models, the RSM is used each and every field to maximize the output. The best thing with the RSM is that it easily converts the responses in terms of the explanatory variables by 2nd order model. The model accuracy has been determined based on the various error factors and validated with the actual experimental setup.

In this analysis, a Central Composite Design (CCD) has been used for defining the input variables and total number of the run. The CCD based on two input variables (Solar Flux, Discharge) [48], code and coded values of the input variables are given in Table 6, the total number of the runs is 13 in which, cube points are 4, center points in the cube are 5 and axial points in the cube are 4 as shown in Figure 5. Table 3 represents the total number of experimental runs and corresponding responses. The variable α represents the rotatibility of the matrix and it is determined by the following equation.

Table 5. Properties of the several layers of the solar panel

Materials	Density (Kg/m^3)	Thermal Conductivity (W/m. k)	Specific Heat Capacity (J/kg. K)
ETFE	1730	0.24	1172
EVA	945	0.35	2090
Silicon	2330	148	700
PET	1350	0.275	1275
CFRP	1490	6.83	1130
Tape	1012	0.19	2000

$$\alpha = \left(2^k\right)^{\frac{1}{4}} \quad (30)$$

Where k represents the number of factors. In the two factors design k = 2, then α = 1.414. In CCD design, based on the total number of the runs, the responses have been calculated and with the help of the ANOVA analysis 2nd order polynomial has been generated. The 2nd order polynomial of response variables have been represented by following equation [49].

$$Y = A_\circ + \sum_{i=1}^{k} A_i x_i + \sum_{i=1}^{k} A_{ii} x_i^2 + \sum_{j\geq 1}^{k} A_{ij} x_i x_j + B \quad (31)$$

The x_i and x_j are the input variables and Y is the dependent variable. A_0, A_i, A_{ii} and A_{ij} are the constant of the linear and square terms. The B represents the error or the noise in the model equation. Based on the data of the Table 3, the following model equations have been developed for the responses namely module temperature (Tm), power output (W), solar panel efficiency (η_P) and exergy efficiency (η_{eX}).

$$T_m = -44.12 + 0.2420S - 707Q - 0.000122S^2 + 3633Q^2 + 0.298SQ \quad (32)$$

$$W = 1.2827 + 0.007098S + 4.69Q - 0.000002S^2 + 50Q^2 + 0.01586SQ \quad (33)$$

$$\eta_P = 20.471 - 0.02178S + 63.6Q + 0.000011S^2 - 327Q^2 - 0.0268SQ \quad (34)$$

$$\eta_{eX} = 22.317 - 0.02375S + 69.4Q + 0.000012S^2 - 356Q^2 - 0.0292SQ \quad (35)$$

Based on these model equations error of all the responses has been calculated and the model has been validated with experimental data. Table 7, Table 8, and Table 9 represents the error analysis of the responses. In Table 7 and Table 8, the P values of all responses are less than 0.01 showing the model is significant. Table 9 shows the values of the R^2, adjusted R^2 and predicted R^2 values which are larger than 0.75 shows the model is best fitted with this data.

Figure 6 represents the residual plots for all data sets of

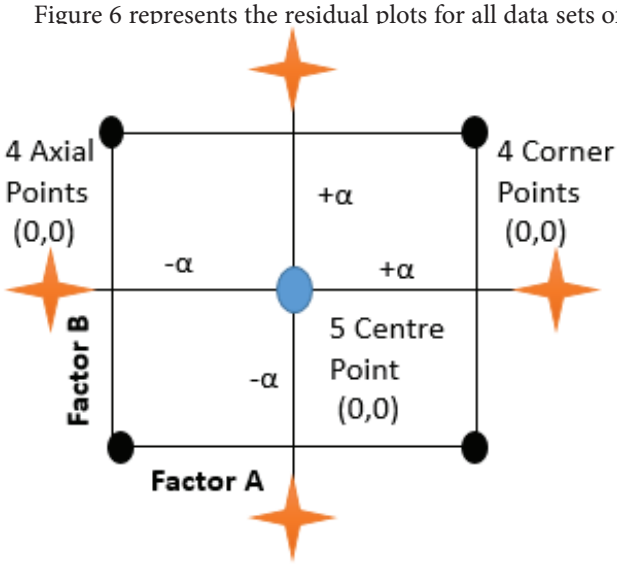

Figure 5. Location of the points in CCD design for two factors [49].

Table 6. Numerical values of the input variables

Input Variables	Coded Level		
	-1	0	1
Solar Flux (W/m²)	400	600	800
Air Discharge (m³/s)	0.01	0.015	0.02

the responses. Residual is the difference between the actual value and the predicted average value obtained by ANOVA analysis. If the value of the particular data point is greater than the average value of the response, the residual is positive [50, 51]. If the value of particular point value is less

Table 7. P-values and F-values for ANOVA analysis on module temperature (Tm) and power output of solar panel (P)

		Silicon Cell Temperature (TC)					Power Output (P)				
Sources	**DF**	**Adj. SS**	**Adj. MS**	**F-value**	**P-value**	**Significant**	**Adj. SS**	**Adj. MS**	**F-value**	**P-value**	**Significant**
Model	5	3397.2	679.44	998.26	<0.0001		8.60	1.72	37987.13	< 0.0001	
S	1	3191.74	3191.74	4689.43	< 0.0001		8.51	8.51	1.880E+05	< 0.0001	
m	1	35.22	35.22	51.75	0.0002		0.0494	0.0494	1090.25	< 0.0001	
S*S	1	166.1	166.14	244.09	< 0.0001		0.0367	0.0367	810.79	< 0.0001	
m*m	1	0.057	0.0574	0.0843	0.7800		0.0000	0.0000	0.2407	0.6387	
S*m	1	0.354	0.3541	0.5202	0.4941		0.0010	0.0010	22.23	0.0022	
Error	4.76	1.80	0.6806	-	-		0.0003	0.0000	-	-	
Lack of Fit	4.76	1.80	1.59	17982.92	0.000		0.0003	0.0001	30784.03	0.000	
Pure Error	0.00	0.00	0.000	-	-		0.0000	0.0000	-	-	
Total	12	3401.96	-	-	-		8.60	-	-	-	

Table 8. P-values and F-values for ANOVA analysis on solar panel efficiency (η_P) and exergy efficiency (η_{eX})

		Solar panel Efficiency (η_P)					Exergy Efficiency (η_{eX})				
Sources	**DF**	**Adj. SS**	**Adj. MS**	**F-value**	**P-value**	**Significant**	**Adj. SS**	**Adj. MS**	**F-value**	**P-value**	**Significant**
Model	5	27.52	5.50	998.26	<0.0001		32.70	6.54	998.26	< 0.0001	
S	1	25.85	25.85	4689.43	< 0.0001		30.72	8.51	4689.43	< 0.0001	
m	1	0.2853	0.2853	51.75	0.0002		0.3391	0.0494	51.75	0.0002	
S*S	1	1.35	1.35	244.09	< 0.0001		1.60	1.60	244.09	< 0.0001	
m*m	1	0.000	0.0005	0.0843	0.7800		0.0006	0.0006	0.0843	0.7800	
S*m	1	0.002	0.0029	0.5202	0.4941		0.0034	0.0034	0.5202	0.4941	
Error	7	0.038	0.0055	-	-		0.0459	0.0066	-	-	
Lack of Fit	3	0.038	0.0129	17982.92	0.000		0.0459	0.0153	-	0.000	
Pure Error	4	0.00	0.000	-	-		0.0000	0.0000	-	-	
Total	12	27.56	-	-	-		32.75	-	-	-	

Table 9. Error Analysis of the responses

Error	**Module Temperature**	**Power Output**	**Solar Panel Efficiency**	**Solar Panel Exergy Efficiency**
Std. Dev.	0.8250	0.0067	0.0742	0.0809
Mean	47.04	5.07	12.27	13.37
C.V. %	1.75	0.1327	0.6053	0.6053
R^2	0.9986	1.0000	0.9986	0.9986
Adjusted R^2	0.9976	0.9999	0.9976	0.9976
Predicted R^2	0.9900	0.9997	0.9900	0.9900
Adeq Precision	100.7990	638.2172	100.7990	100.7990

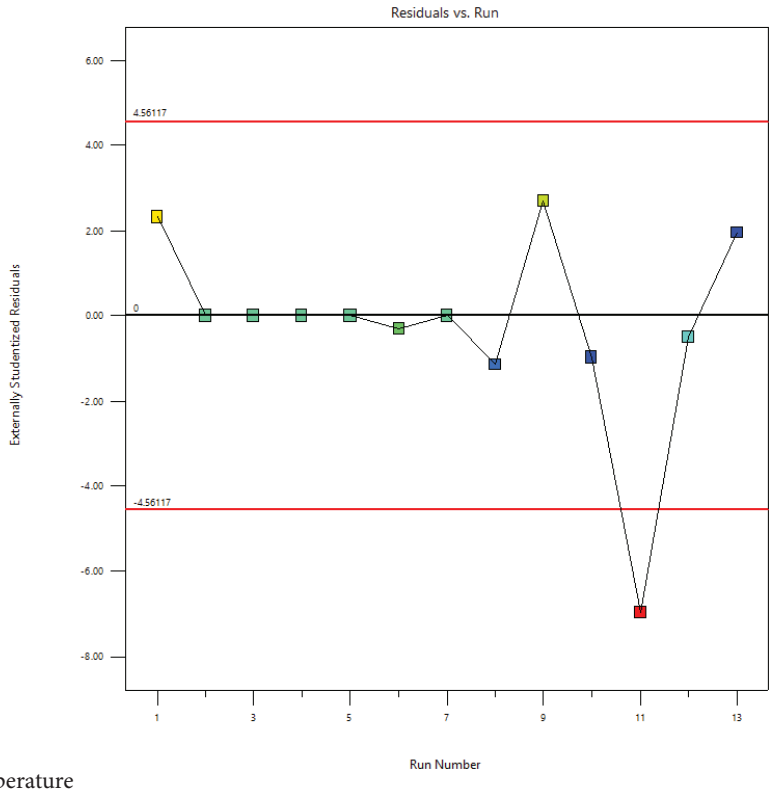

(a) Residual plot of module temperature

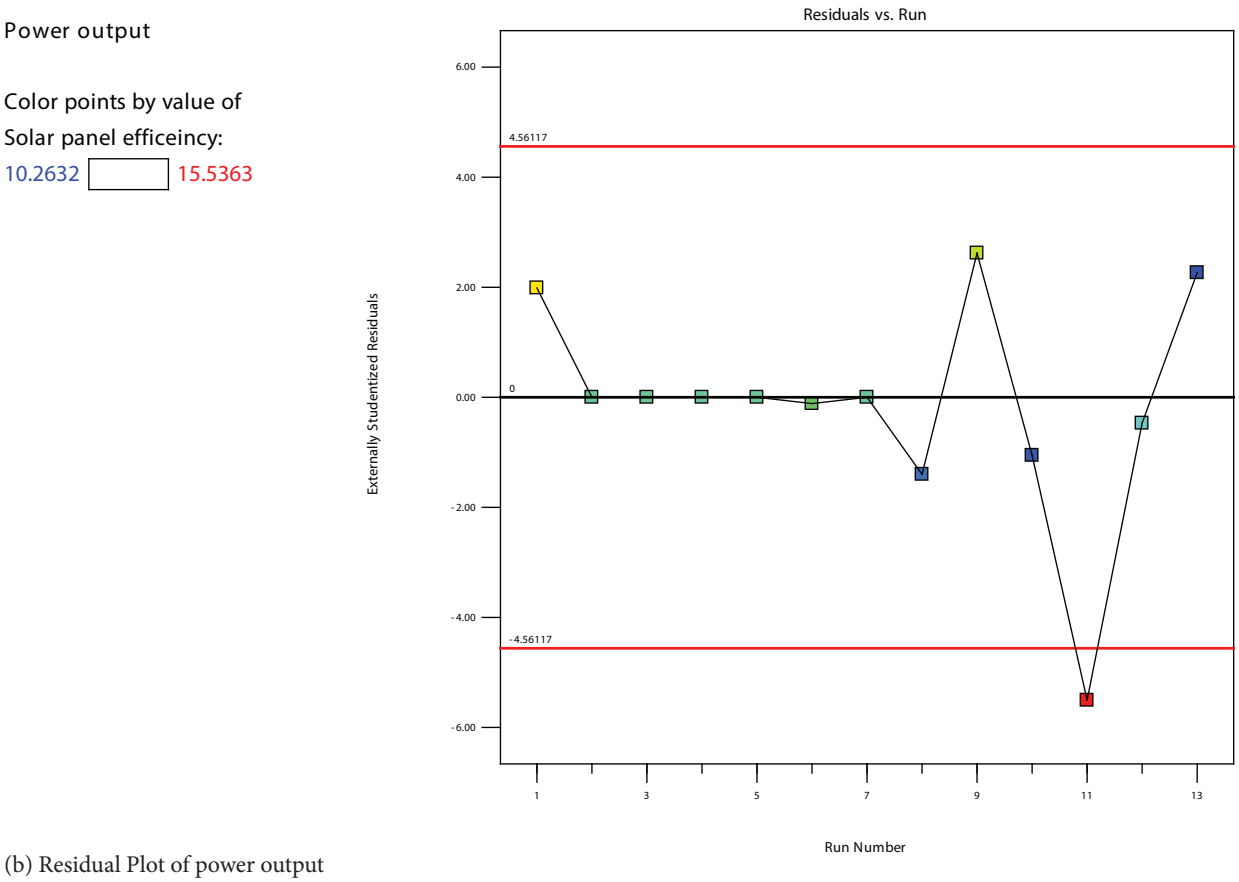

(b) Residual Plot of power output

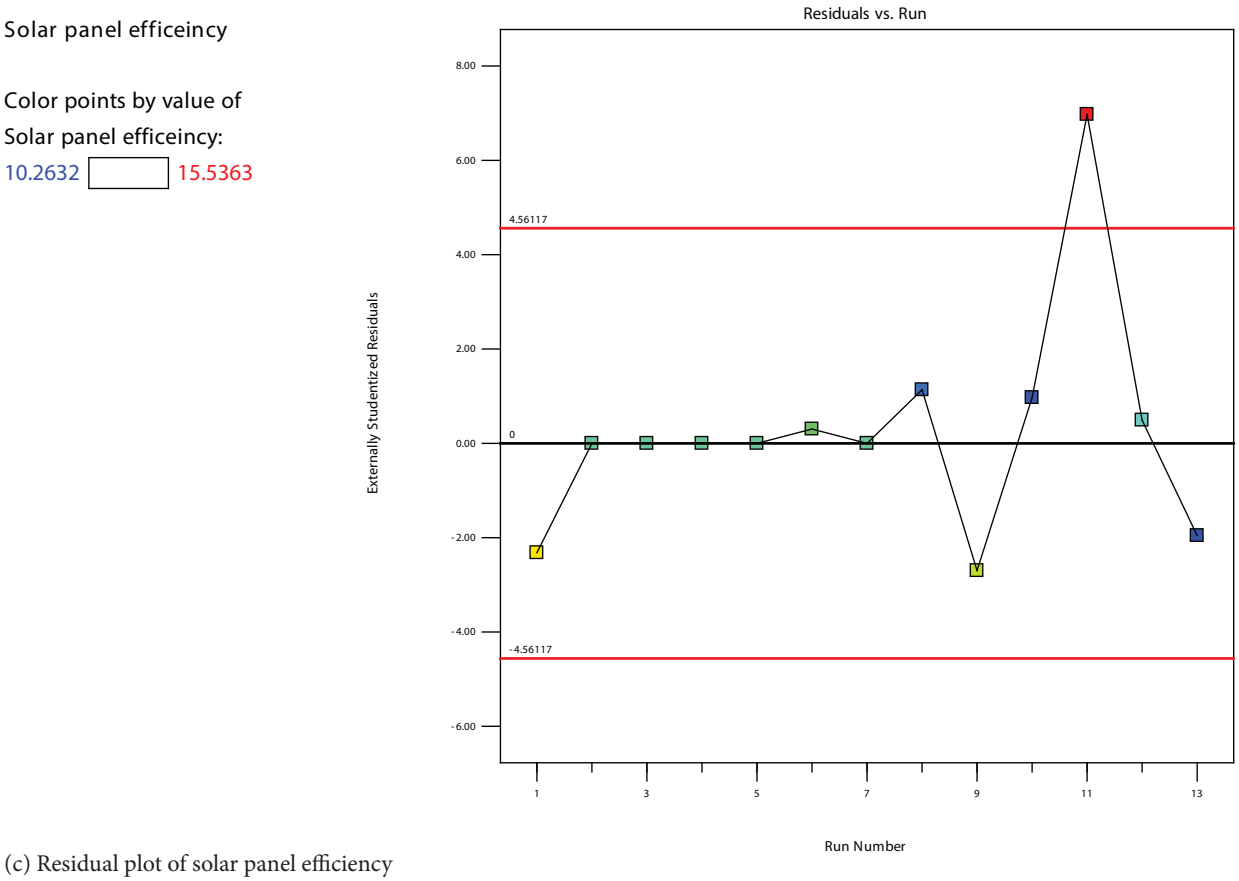

(c) Residual plot of solar panel efficiency

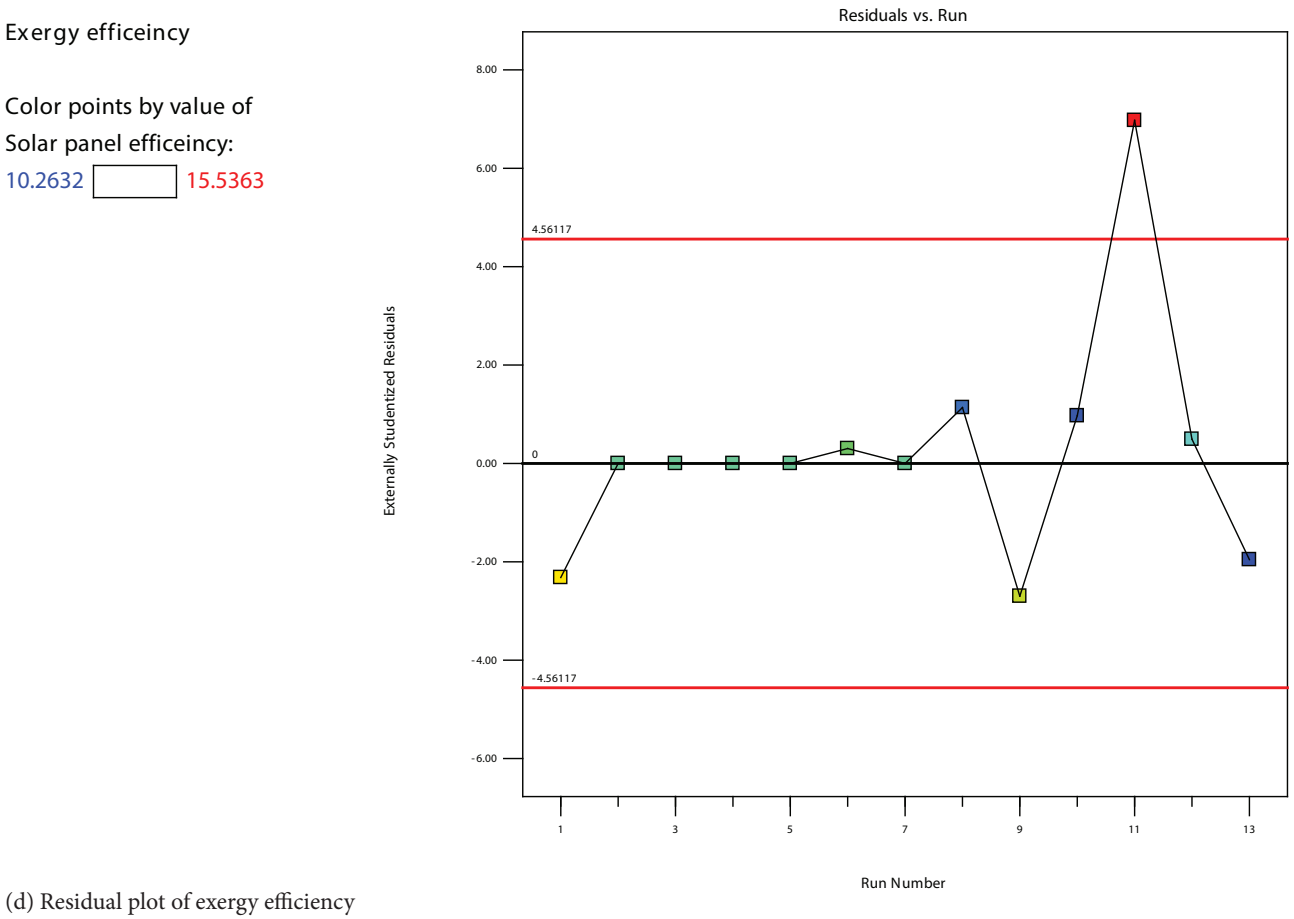

(d) Residual plot of exergy efficiency

Figure 6. Residual plot of the response parameters.

than the average value of the response, the residual is negative. So, for all runs, the sum of the residuals is zero. Figure 6 (a), Figure 6(b), Figure 6 (c), and Figure 6 (d) show that the residual of all responses is maximum at 11 run or data set since the solar flux at 11 run is very less only 317 W/m^2 beyond the range of the solar flux 400 W/m^2 to 800 W/m^2. It is clearly indicated from Figure 6 (a), Figure 6 (b), Figure 6 (c), and Figure 6 (d), the all data sets are well organised about the average line which shows the accuracy of the responses.

Figure 7 shows the perturbation plots of the responses concerning the input variables. The perturbation plots depicted, the behaviour of the response variable by treating the input variables at constant variables. Figure 7 (a) shows the value of the reference point to be (0.00, 49.85°C). In Figure 7 (a), if a point on the curve moves far from the reference point, a steep change in the graph of solar flux is to be noted at the constant value of the air discharge which shows, the sensitivity of module temperature with solar flux. The lower and constant slope of line B represents the lower sensitivity with air flow rate. Figure 7 (b) reference point is (0.00, 4.95 Wp) and the slope of the solar flux curve and air flow rate curve have constant values since both lines are straight in nature [52].

It indicates that solar flux and air flow rate both constantly affect the power production of solar panel. Figure 7 (c) shows, the intersection coordinate of both curves A and B is (0.00, 12%) gives the optimum value of the solar panel efficiency [53]. The solar flux steep change of the graph at constant discharge shows the solar flux is further likely to affect the solar panel efficiency as compared to the air flow rate. On other hand, the discharge line B slope remains constant give the indication that, the solar panel efficiency constantly changes with the discharge of air. Figure 7 (d) shows the perturbation plots of exergy efficiency of solar panel. Figure 7 (d) reference point is (0.00, 13.01%). Curve A (solar flux) higher steep changes in slope shows, the sensitivity of solar flux with the exergy efficiency at a constant value of the air flow rate, and the lower and constant variation in line B slope (Air flow rate) shows lower sensitivity with the exergy efficiency [54].

RESULTS AND DISCUSSION

Module Temperature Variation with Input Variables

Figure 8 shows the 3D plots of the module temperature with solar flux and air flow rate in which if the solar

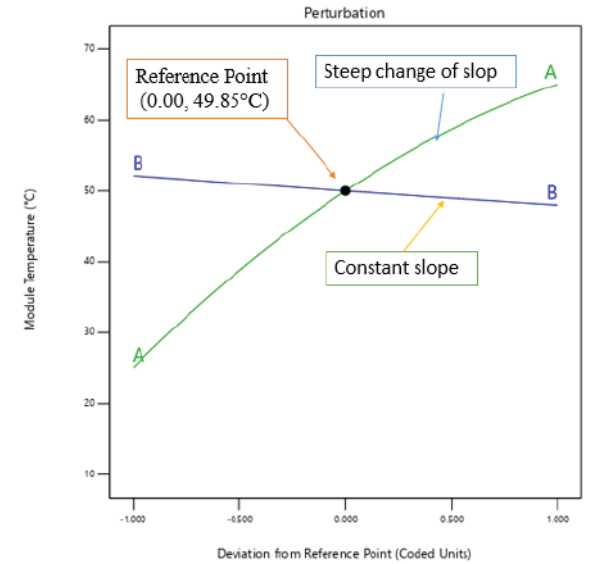

(a) Perturbation plot of the module temperature

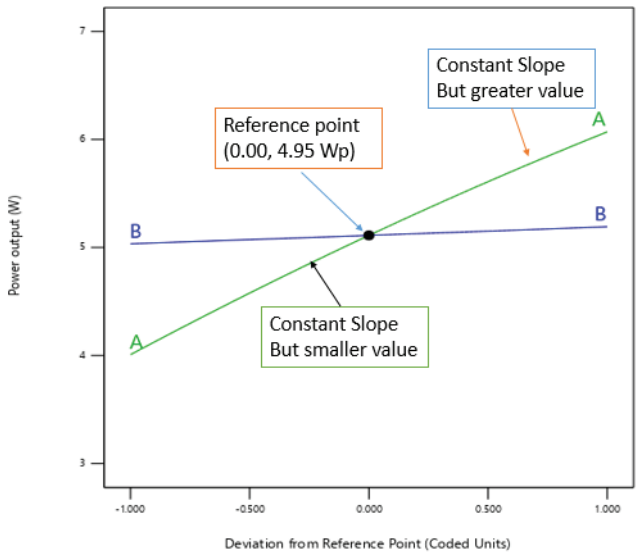

(b) Perturbation plot of the power output

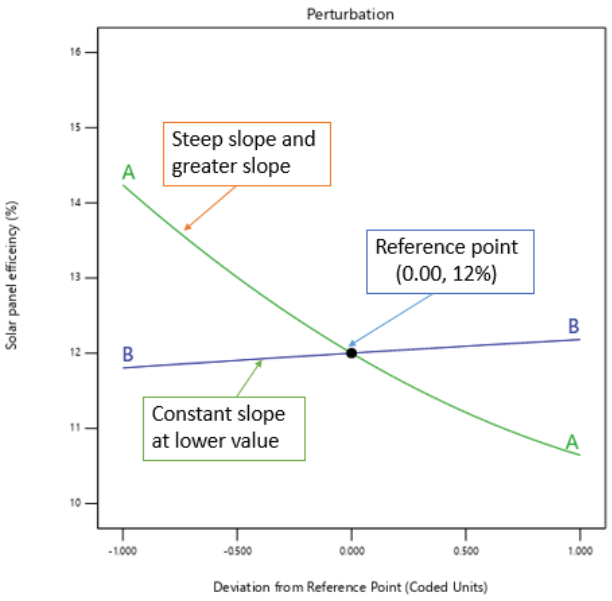

(c) Perturbation plot of the solar panel efficiency

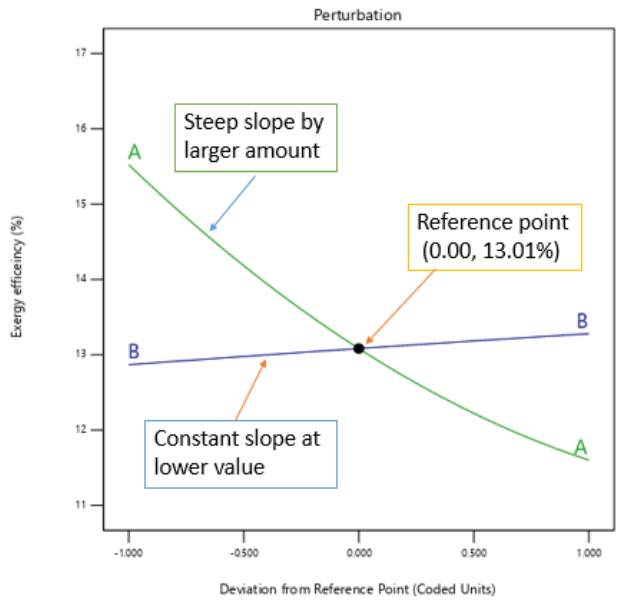

(d) Perturbation plot of the exergy efficiency

Figure 7. Perturbation plot of the responses with respect to input variables.

flux increases then the module temperature increases sharply due to the supply of higher solar energy on the surface of the solar panel. The higher energy content enhanced the trapped heat inside the solar panel which will increase the solar panel temperature. On the another hand with air flow rate, the module temperature is reduced due to an increase of mass flow rate since at higher mass flow rate more heat is carried by the air which lowers the module temperature [55]. Figure 8 indicates that the module temperature is 27.6°C at the solar flux of 400 W/m^2 and it increased to 67.1°C at the solar flux of 800 W/m^2. The 58.9% hike in module temperature occur due to two times increasing the solar flux. Figure 8 also shows that if the solar flux is more than 720 W/m^2, the module temperature is higher than 60°C. So, at higher solar flux air flow rate should be more than 0.02 m^3/sec [56] which enumerated that at high solar flux systems cooling is very much required to sustain the efficiency of the solar panel.

Power Output of Solar Panel with Input Variables

Figure 9 shows the trend of the power output with solar flux and air discharge. It is seen from the figure that if the solar flux is enhanced, the solar panel's power output is enhanced due to the supply of the higher solar energy [51], [57]. The solar panel's power output is increasing as

the air flow rate increases, due to a reduction in the module temperature leading to an increase in the efficiency of the solar panel. As the airflow rate increases, the mass flow rate increases which carries a higher amount of heat to cool down the solar panel. The cooling of solar panel enhances the output power. The increased air discharge also increases energy consumption so it is not always advantageous to increase the air discharge. It is true up to the optimum values of the discharge, after crossing the optimum condition, the power consumption by the fan is greater than the power production of the solar panel which reduces the net efficiency of the solar panel.

Solar Panel Efficiency Variation With Input Variables

Figure 10 denotes the solar panel efficiency with respect to the solar flux and the airflow rate. Figure 10 clearly shows that as the solar flux increases, the solar panel efficiency is enhanced due to an growth in power output with the solar flux [58]. As the solar flux increases,

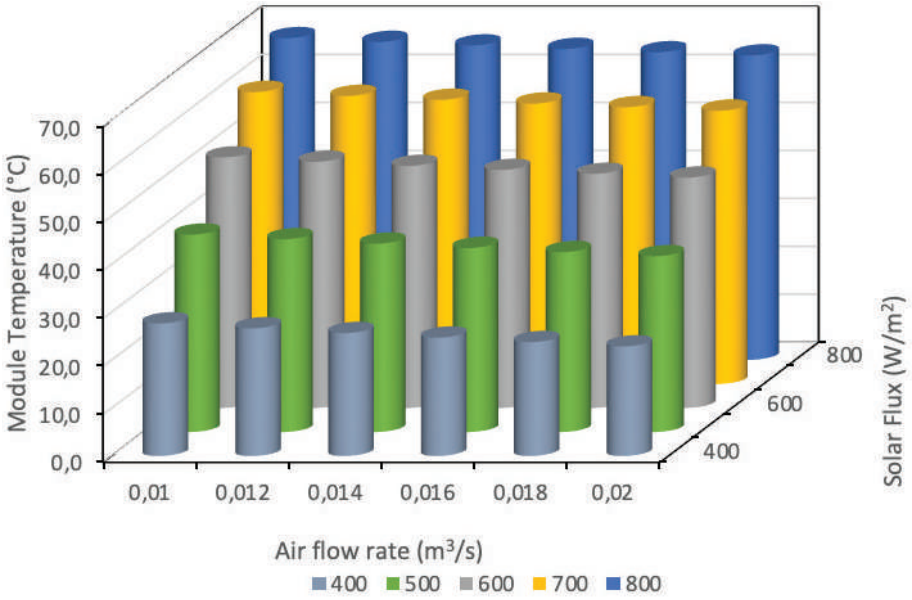

Figure 8. Temperature variation of solar panel with input variables.

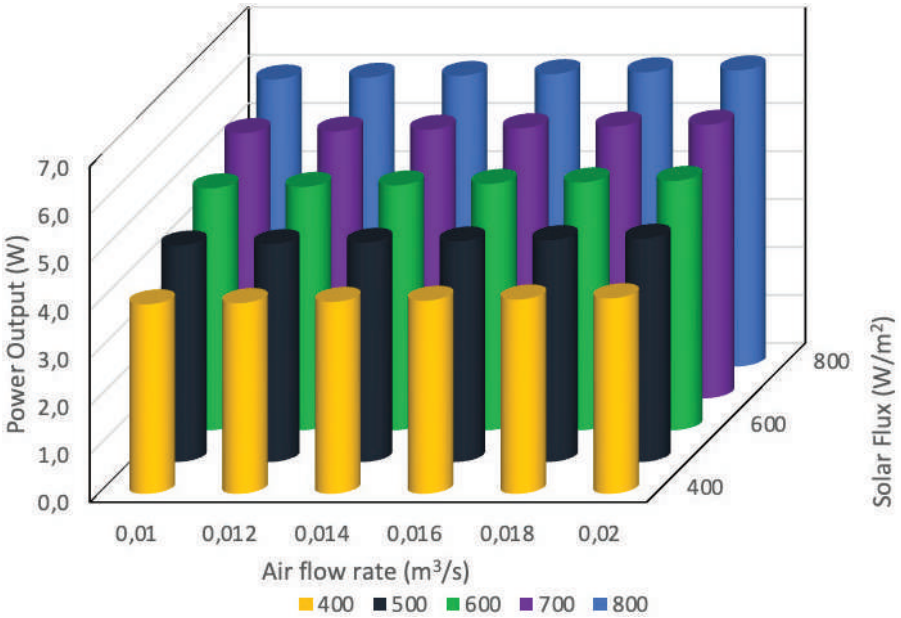

Figure 9. Power output variation of solar panel with input variables.

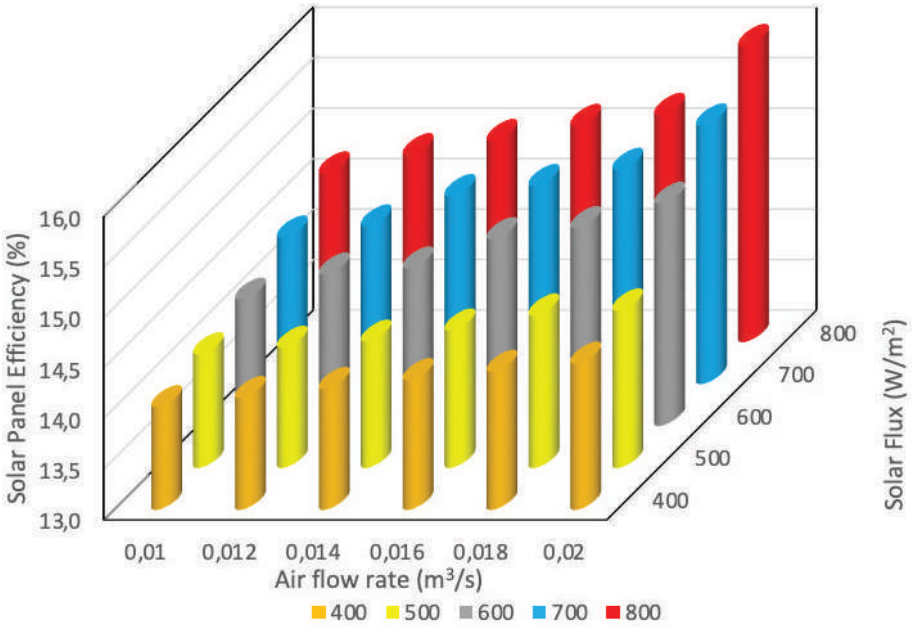

Figure 10. Solar panel efficiency variation with input variables.

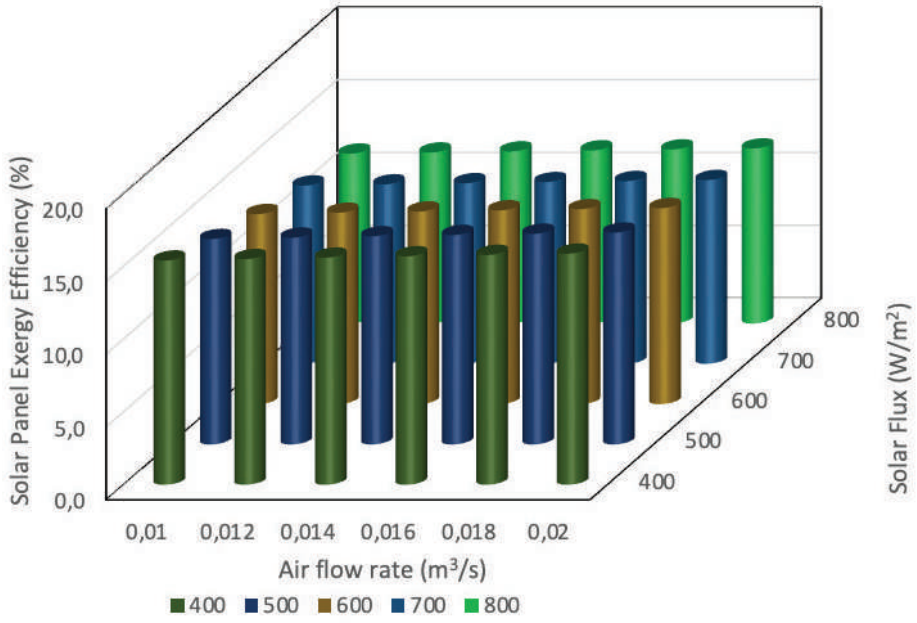

Figure 11. Solar panel exergy efficiency variation with input variables.

the module temperature too increases but enhancement of power output due to the intensity of solar flux is more dominating as compared to reduction of the power output of solar panel due to enhancement of the module temperature. So, the overall outcome is an increase in the efficiency of solar panels due to an increase in solar flux intensity. The solar panel efficiency variation with air discharge is an increasing trend due to the reduction in solar panel temperature. As the air discharge increases more heat is carried by the air which enhances the heat-carrying capacity of air. The cooled solar panel gives higher solar panel efficiency as compared to without cooled solar panels. Increasing the air discharge also increases the fan input power so net efficiency starts to reduce after reaching the optimum values. So, it is not always advantageous to enhance the air discharge.

Solar panel exergy efficiency variation with input variables

Figure 11 represents, the exergy efficiency of the solar panel with respect to the solar flux and discharge of air. Figure 11 trends of the exergy efficiency show that if the solar flux rises then the exergy efficiency declines [59] since an increase in solar flux increases the module temperature of the solar panel. The exergy efficiency is represented by equation number (25), so from this equation, it can be observed that if the solar flux increases, the input exergy increases which reduces the exergy efficiency. The input exergy is the sun of the solar exergy and fan input electric work. Figure 11 exergy efficiency variation with air discharge shows that if the air discharge increases then the exergy efficiency of the solar panel increases. The exergy efficiency of the solar panel increases with air discharge since at a higher air mass flow rate, the cooling effect of the solar panel is enhanced and the module temperature of the solar panel is reduced [60]. However, increasing the air discharge also enhances the fan input exergy so always increasing the air discharge do not enhance the exergy efficiency.

LCOE of the solar panel

Figure 12 depicts the LCOE of the finned solar panel and without the finned solar panel. it is seen from Figure 12, the LCOE of the without-finned solar panel is 2.4033 INR/kWh, and with finned solar panel is 2.21 INR/kWh. The 8.75 % reduction in LCOE has been noted due to the chilling of solar panels by air. The LCOE is measured to compare the cost required to produce the 1 unit of the electricity. Moreover, figure clearly show that the cost of production of the electricity is only 2.21 INR/kWh in the finned solar air heater. This data is for the 10 Wp solar panel, if the size of the solar panel enhanced then the LCOE is reduced due to production of the more power by the solar panel.

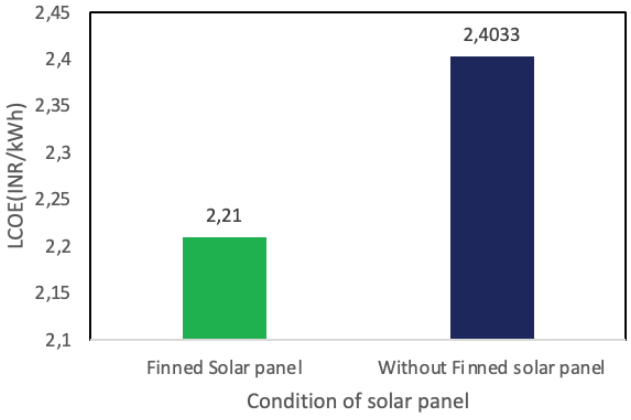

Figure 12. LCOE of the solar panel with and without fins.

Optimum Values of The Responses with Input Variables

Figure 13 illustrates, the optimization plots of the responses with respect to the input variables, this figure shows the ranges of input variables, optimum values of input variables, optimum value of response variables, and composite desirability of the optimization. Figure 13 depicts, the optimum values of the input variables namely solar flux and air discharge is 403.3586 W/m^2 and 0.0221 m^3/sec on which responses exergy efficiency 15.781%, the power production of the solar panel 4.1196 Wp, module temperature 22.4279°C and solar panel efficiency 14.4815%. The red colour numbers indicate, the optimum values of the input variables and blue colour words represents the optimum values of the output variables.

The desirability represents, the correlation among input and output variables. The individual desirability and the composite desirability of the input and response variables are given in Figure 12. The composite desirability of the optimization plots is given as 0.5737 and the individual desirability of responses exergy efficiency, power output, module temperature, and the solar panel efficiency is namely 0.79996, 0.2164, 0.79996, and 0.79996.

Validation of the model

The optimum condition obtained by the optimization process has been validated by running the experimental setup. Three consecutive test has been conducted and the average value of the responses corresponding optimum values of the solar flux (403.3586 W/m^2) and air flow rate (0.02 m^3/s). Table 10 represents the predicted values through the models, experimental average values of responses and percentage error.

Percentage Change in Performance of Air Cooled Solar Panel with Respect to Simple Solar Panel

Figure 14 shows the percentage change in module temperature, power output, solar panel efficiency, and exergy

Table 10. The verification test of output response

	Predicted value	Experimental value	Error (%)
Module Temperature (°C)	22.42	21.63	3.5%
Fan power output (W)	4.1196	3.963	3.8%
Solar Panel Efficiency (%)	14.48	13.94	3.67%
Solar panel Exergy Efficiency (%)	15.7871	15.2997	3.1%

Solar Flux (403.3586 W/m^2) and Discharge (0.0221 m^3/s)

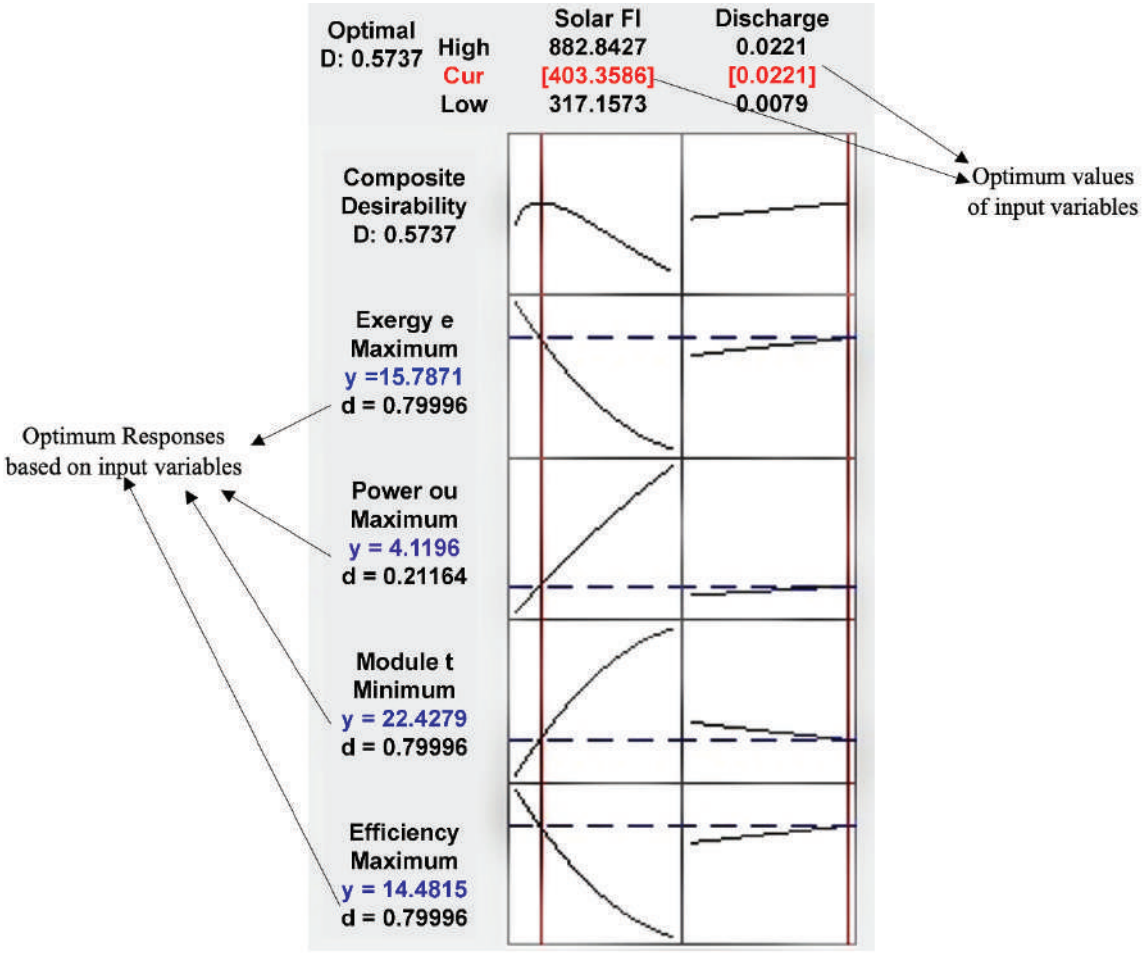

Figure 13. Desirability, optimum values of the inputs and responses.

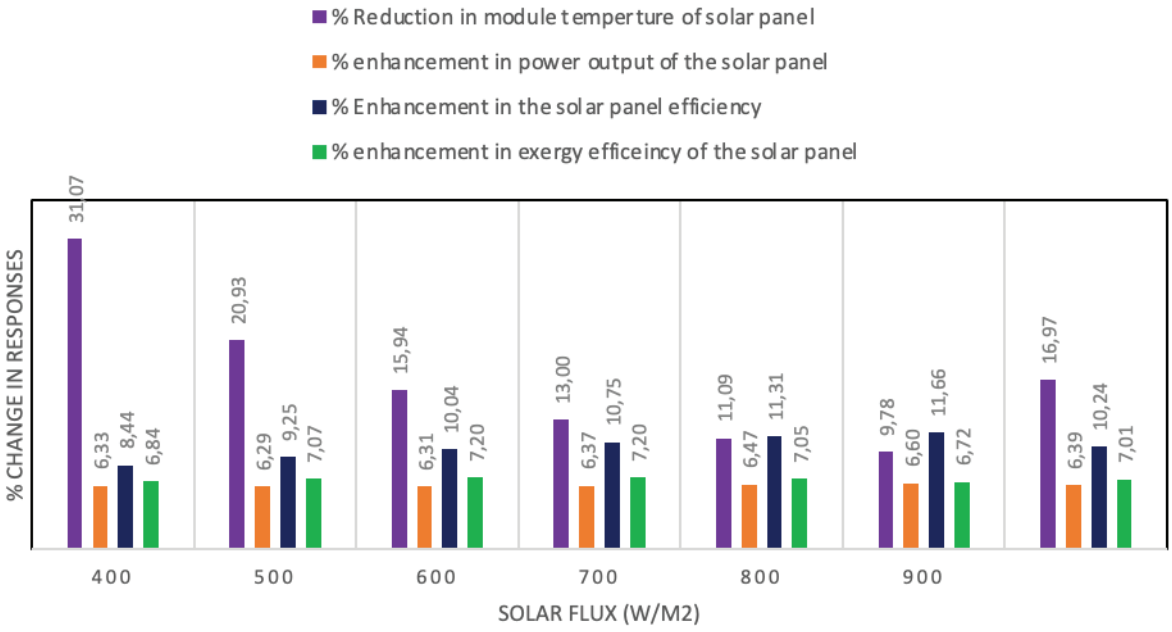

Figure 14. Solar panel performance enhancement due to air cooling as compared to without cooled system.

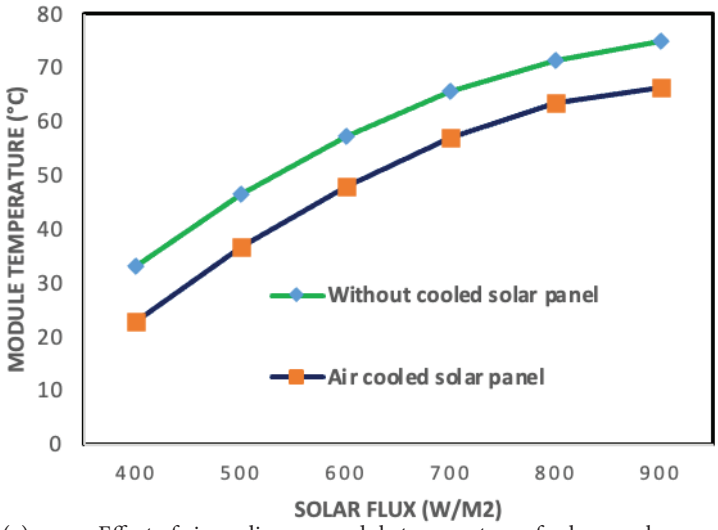

(a) Effect of air cooling on module temperature of solar panel

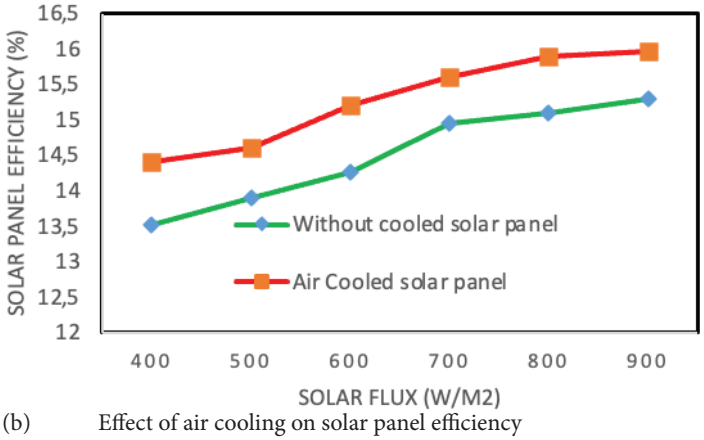

(b) Effect of air cooling on solar panel efficiency

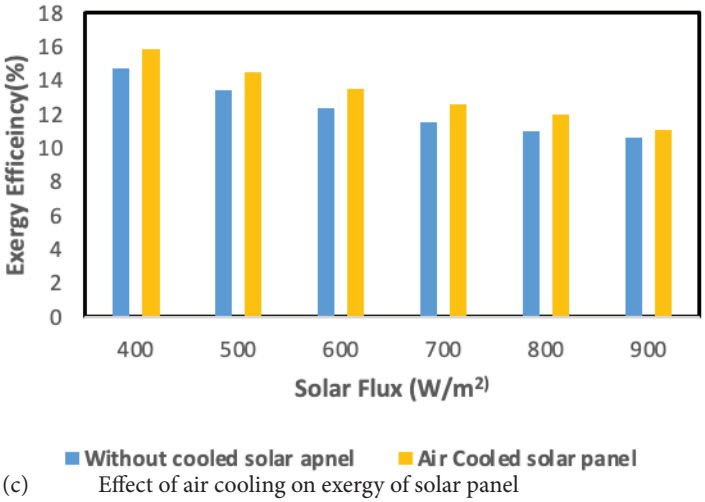

(c) Effect of air cooling on exergy of solar panel

Figure 15. Comparison of module temperature, solar panel efficiency and solar panel exergy with air or without air cooled solar panel.

efficiency of air-cooled solar panel at an air discharge of 0.02 m^3/s. The percentage reduction of the module temperature of the solar panel depicts that as the solar flux increases then the reduction in module is less since at the higher solar flux air cooling is not sufficient to lower down the module temperature. Figure 14 clearly shows that as the solar flux increases then the percentage change in the power production of the solar panel increased since at the higher solar flux the input energy supplies increased which will further enhance the power output of the solar panel.

The solar panel efficiency also enhanced as the solar flux increased at the air discharge 0.02 m^3/s, the percentage change of the solar panel efficiency is higher at the higher solar flux. The exergy efficiency percentage growth with solar flux increases initially but after reaching to optimum solar flux, the exergy efficiency starts to reduce since augmentation in the solar flux raises the module temperature which reduces the exergy efficiency of the solar panel.

Figure 15 illustrates the comparison between the air cooled and without cooled solar panel performance. Figure 15 (a) depicts that if the soar flux increasing, the module temperature of the soar panel always increasing trends. The maximum module temperature of without cooled and with air cooled solar panel are noted to be 74.86°C and 66.25°C at air flow rate of the 0.02 m^3/s and solar flux 900 W/m^2. Figure 15 (b) display the percentage variation of the solar panel efficiency with the solar flux. As the solar flux increasing, the power production through the solar panel enhanced which increase the solar panel efficiency. Figure 15 (c) shows the exergy efficiency variation with the solar flux. As the solar flux increasing, the exergy efficiency reduces due to increase in the solar panel temperature at higher solar flux. The maximum exergy efficiency obtained to be 15.9% and 14.73% at the solar flux of 400 W/m^2 and 0.02 m^3/s discharge.

Validation of the Results

The results of the current study are validated with the Anurag et al. (2022) [61]. Anurag et al. (2022) performed the experimental and numerical of the air-cooled solar panel by various configurations of the fins produced below the surface of the solar panel. Table 11 shows the variation of the solar flux, solar panel temperature, and solar panel efficiency variation for the longitudinal fins in tabular form. Figure 16 illustrates the validation of the results of the current study with the Anurag et al. (2022) [61]. Figure 16 (a) depicts reasonable agreement between the surface temperature variation of current research with Anurag et al. (2022). Both studies agreed that as the solar flux growths, the solar panel surface temperature increases. The current study showed that at the solar flux of 1100 W/m^2, the maximum temperature reached to 68.32°C which is very near to the 67.32°C solar panel surface temperature of Anurag et al. (2022). Figure 16 (b) also displays that the solar panel efficiency increases as the solar flux increases. The maximum efficiency of the solar panel is reached to 16.52% and 16.1% in the Anurag et al. (2022) and current study. The cooling of the solar panel is very much required as the solar flux is very high in the summer time in between the 11 AM to 3 PM, in this duration the solar panel performance is drastically reduced but air cooling made this drastic reduction

Table 11. Anurag et al. (2022), solar flux, solar panel surface temperature and solar panel efficiency variation for the longitudinal fins

Time	9 AM	10 AM	11 AM	12 PM	1 PM	2 PM	3 PM	4 PM
Solar Flux (W/m^2)	700	850	1000	1100	1080	910	720	390
Solar Panel Surface Temperature (°C)	55	63.8	69	67.89	66.89	66	56.65	42
Solar Panel Efficiency (%)	15.3	16.1	16.4	16.52	15.1	13.29	13.2	13.12

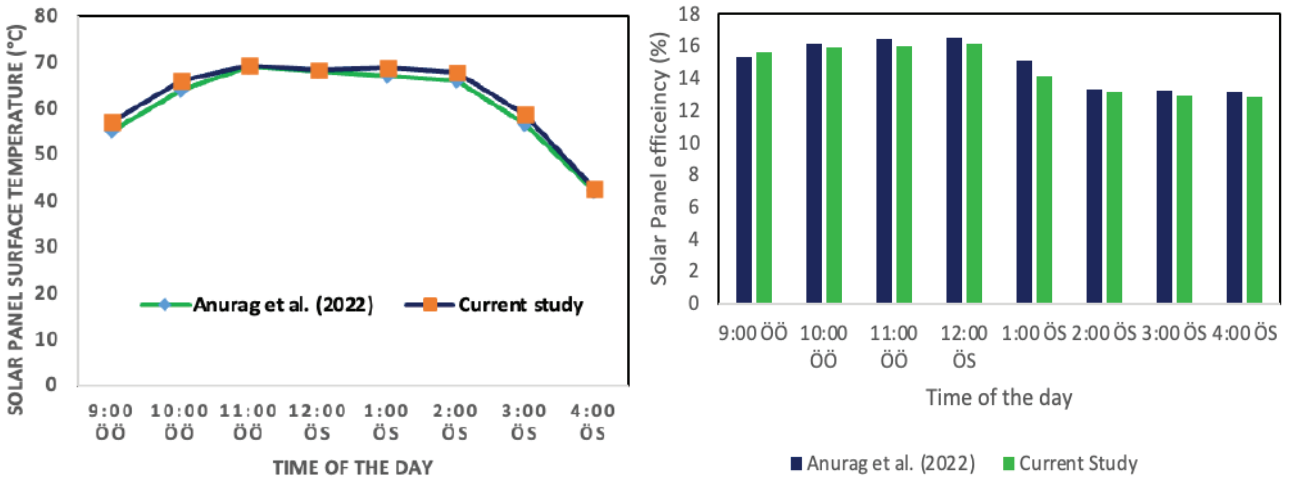

(a) Validation of the surface temperature of the solar panel

(b) Validation of the solar panel efficiency

Figure 16. Validation of the current study with Anurag et al. (2022)

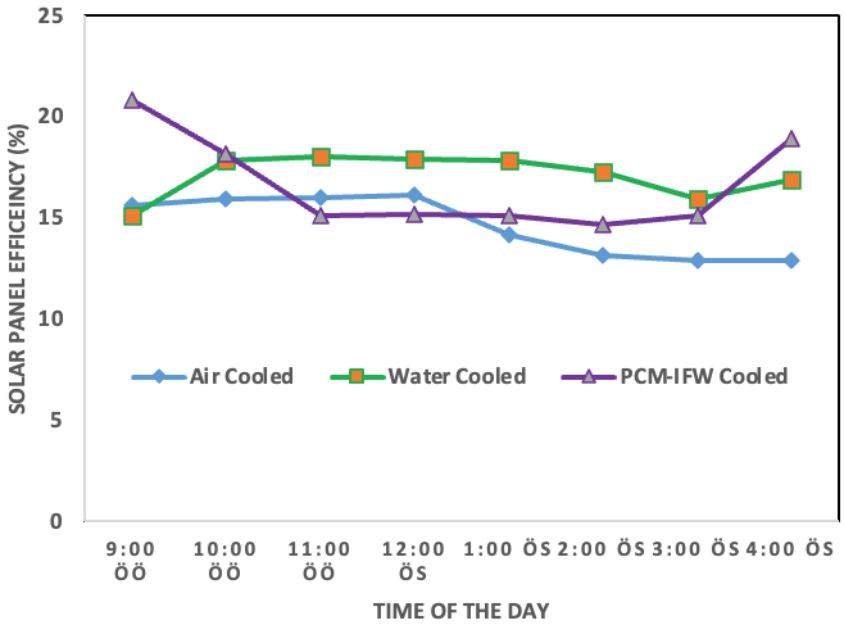

Figure 17. Comparison of the solar panel efficiency with air, water and PCM cooling in summer season.

curve to flatten and maintain the performance of the solar panel within the permissible limit.

Comparison of Air Cooling with the Water and Paraffin Wax with Iron Filling Waste

This section discusses and compares the performance enhancement of solar panel due to the air, water, and PCM-IFW (Iron Filling Waste) cooling. The current research compares with the liquid water cooling [62] and PCM-IFW cooling [63]. Figure 17 depicts that in the morning from 9 AM to 10 AM, the PCM material with IFW gives the maximum efficiency, but after 10 AM to 3 PM, the water cooling at a mass flow rate of 1.5 LPM gives the maximum efficiency. In the morning between 9 AM to 10 AM, the PCM material started to melt and changes the phase, this process absorbs the latent heat and cools down the module at a desirable limit but when all PCM material melted, then it absorbs the sensible heat and lower down the cooling rate and reduce the efficiency. Although, in water cooling, always fresh water at optimum mass flow rate is supplied to the solar panel surface, which maintains the solar panel efficient at a constant level throughout the day. On the other hand, the air has low heat absorbing capacity since air cooling has lower cooling efficiency as compared to the PCM and water cooling.

CONCLUSION

Fossil fuels are exhaustible in nature and not economical due to hikes in price, creating the requirement of alternative fuels that are renewable and eco-friendly to the environment. Solar panel are best fitted to fill this gap since they convert solar energy into electrical energy without creating any harmful effect in the atmosphere. The main drawback of the solar panel is the low performance at high temperatures. So, at the time of the solar panel's working, solar cooling must be required for the sustainability of the efficiency. High solar panel efficiency reduces the initial investment so that it can be afforded by the farmers and the poor people located in rural and remote areas. This research focused on the performance improvement of the solar panel by the use of air cooling. The air cooling is chosen for the study due to its simple arrangement and noncorrosive nature. The main limitation of the study is the lower cooling effect due to the lower thermal diffusivity of the air. However, it is the most used method as a cooling medium in all fields of engineering like automobiles, electronic equipment, and the aerospace industry due to cost-effective and easy of implement. For the thermal analysis of the cooling arrangement, the system has been designed and optimized by the Response Surface Methodology, and the optimum setting of the input and output variables has been determined based on the constraints of the optimization. The percentage enhancement in the responses due to air cooling compared with the without cooled solar panel. The following are the main concluding points of this study.

1. The solar flux and the air mass flow rate are two important input variables that affect the performance of the solar panel. As the solar flux enhanced from 400 W/m^2 to 800 W/m^2, the module temperature augmented from 22.9°C to 63.5°C which hamper the thermal performance from 14.4% to 10.8%.
2. Enhancing the solar flux increases the module temperature of the solar panel due to that the performance

of the solar panel decays throughout the day. The exergy analysis shows that from 400 W/m^2 to 800 W/m^2 increase in solar flux reduces the exergy efficiency from 15.9% to 12.0%.

3. In the optimization process, the optimal solar flux and air discharge were found to be 403.3586 W/m^2 and 0.0221 m^3/s on which responses are module temperature 22.4279°C, power output 4.1196 Wp, PV module efficiency 14.41% and exergy efficiency 15.78%.
4. At higher solar flux and high air discharge is feasible to drop down the temperature of the solar panel since increasing discharge continuously reduces the air temperature. However, at very high temperature of the solar panel, the air cooling will be ineffective in dropping the temperature of the solar panel at the optimum limit, this situation can be handled by using liquid cooling and phase change material. At 800 W/m^2 solar flux if the air discharge increases from 0.01 m^3/s to 0.02 m^3/s, the solar panel efficiency increases from 14.7% to 15.9%.
5. At the discharge of 0.01 m^3/s, the 9.16% reduction in temperature and 3% enhancement in the power output has been recorded and if the discharge is increased to 0.02 m^3/s, the temperature drop is 16.96% and enhancement in power output is 6.39%.
6. The composite desirability of the output and input variables is 0.5737.
7. The R^2, adjusted R^2 and predicted R^2 values are 0.9986, 0.9976, and 0.99 showing the good accuracy of the model generated by analyses of variance.

Role and Significance of the Study

The world›s energy demand is growing day by day. In the current scenario, most of the energy demand has been fulfilled by the use of fossil fuels. The government is focusing on green energy technology which is renewable and free from pollution. Solar panels are the best way of the production of electricity by Sun energy. This study has been performed to enhance the solar panel efficiency to fill the energy demand of the world. The study focused to use the high-density pin fin which can be fixed with the outer plate of the solar panel and air can be blown by the use of the fan. The air cooling is feasible and easily handled.

Limitations of the study and future work

The main limitation of the study is the lower cooling effect due to the lower thermal diffusivity of the air. However, it is the most used method as a cooling medium in all fields of engineering like automobiles, electronic equipment, and the aerospace industry due to cost-effective and easy of implement. This can be overcome by the use of supplying the already-cooled air or supplying the liquid water in dry air at varying concentrations to enhance the heat-carrying capacity of air. The second limitation of air cooling is the noise produced at the time of the flow of the air over the fined surface by the fan or blower. This effect can be mitigated by the use of a partial vacuum in the air duct, using passive techniques, and using the phase change material for cooling the solar panel.

In the future, the research will be focused to know the effect of the humidity in the moist air on solar panel cooling. The system will be optimized to know the effect of the humidity and air dry bulb temperature on the performance of the solar panel. Furthermore, the research will also include cooling the different types of solar panels with PCM, Nano-fluids, and liquid water.

ACKNOWLEDGMENT

The authors thank IFTM University›s management and vice chancellor for permitting them to conduct the study and providing the facilities they needed.

CONFLICT OF INTEREST

The Author’s declare that they have not any conflict of interest.

REFERENCES

[1] Sharaf M, Yousef MS, Huzayyin AS. Review of cooling techniques used to enhance the efficiency of photovoltaic power systems. Environ Sci Pollut Res 2022;29:26131–26159. [Crossref]

[2] Teo HG, Lee PS, Hawlader MNA. An active cooling system for photovoltaic modules. Appl. Energy 2012;90:309–315. [Crossref]

[3] Choi SM, Kwon HG, Kim T, Moon HK,Cho HH. Active cooling of photovoltaic (PV) cell by acoustic excitation in single-dimpled internal channel. Appl Energy 2021;309:118466. [Crossref]

[4] Deivakumaran S, Chua YL, Koh YY. Active cooling system for solar panels with silver nanofluid and water. IOP Conf Ser Earth Environ Sci 2023;1205. [Crossref]

[5] Tonui JK, Tripanagnostopoulos Y. Performance improvement of PV / T solar collectors with natural air flow operation. 2008;82:1–12. [Crossref]

[6] Yun GY, Mcevoy M, Steemers K. Design and overall energy performance of a ventilated photovoltaic façade. 2007;81:383–394. [Crossref]

[7] Nuwayhid RY. Thermal analysis of photovoltaic-thermoelectric hybrids. J Therm Eng 2024; 10:1149–1163. [Crossref]

[8] Gelis K, Al-Khatib OA, Ozbek K. Development of partitioned rectangular-shaped heat sink for photovoltaic thermal systems and performance evaluation using TiO2/Water-based nanofluids. Appl Therm Eng 2024;248:123220. [Crossref]

[9] Gelis K, Celik AN, Ozbek K, Ozyurt O.Experimental investigation into efficiency of SiO2/water-based nanofluids in photovoltaic thermal systems using response surface methodology. Sol Energy 2022;235229–241. [Crossref]

[10] Vithanage V, Hosan S, Perera H, Galpaya C, Induranga A. Impact of water based nanofluids in heat exchanger type active solar PV cooling systems : A comparative CFD analysis. 2025.
[11] Sheikh Y, Jasim M, Qasim M, Qaisieh A, Hamdan MO, Abed F. Enhancing PV solar panel efficiency through integration with a passive Multi-layered PCMs cooling system: A numerical study. Int J Thermofluids. 2024;23:100748. [Crossref]
[12] Sudhakar P, Santosh R, Asthalakshmi B, Kumaresan G, Velraj R. Performance augmentation of solar photovoltaic panel through PCM integrated natural water circulation cooling technique. Renew Energy 2021;172:1433–1448. [Crossref]
[13] Akkoyunlu MT, Abdallatif Y. A comprehensive investigation of solar panel cleaning technologies: A review study. J Therm Eng 2024;10:1715–1741. [Crossref]
[14] Hasan A, McCormack SJM, Huang J, Norton B. Characterization of phase change materials for thermal control of photovoltaics using Differential Scanning Calorimetry and Temperature History Method. Energy Convers Manag 2014;8:322–329. [Crossref]
[15] Stropnik R, Stritih U. Increasing the efficiency of PV panel with the use of PCM. Renew Energy 2016;97:671–679. [Crossref]
[16] RM, LS, RS, AH, DA. "Experimental investigation on the abasement of operating temperature in solar photovoltaic panel using PCM and aluminium. Sol Energy 2019;188 327–338:2019. [Crossref]
[17] Alzgool M.Performance Enhancement by Cooling the PV Panels Using Phase Change Material (RT35): ANSYS Simulation and Experimental Investigation. Int J Energy Prod Manag 2024;9:73–81. [Crossref]
[18] Madurai Elavarasan R, Nadarajah M, Pugazhendhi R, Gangatharan S. An experimental investigation on coalescing the potentiality of PCM, fins and water to achieve sturdy cooling effect on PV panels. Appl Energy 2023;356:122371. [Crossref]
[19] Golzari S, Kasaeian A, Amidpour M, Vatan SN, Mousavi S. Experimental Investigation of the Effects of Corona Wind on the Performance of an Air-Cooled PV/T. Renew Energy 2018. [Crossref]
[20] Alrobaian AA. Performance of PV panel coupled with geothermal air cooling system subjected to hot climatic. 2017;148:1–9. [Crossref]
[21] Arifin Z, Danardono D, Prija D, Hadi S. Numerical and Experimental Investigation of Air Cooling for Photovoltaic Panels Using Aluminum Heat Sinks 2020;2020. [Crossref]
[22] Lebbi M, Baissi MT, Hassani S. Energy performance improvement of a new hybrid PV / T Bi-fluid system using active cooling and self-cleaning : Experimental study. Appl Therm Eng 2020;116033. [Crossref]
[23] Salehi R, Jahanbakhshi A. Reza Golzarian M, Khojastehpour M. Evaluation of solar panel cooling systems using anodized heat sink equipped with thermoelectric module through the parameters of temperature, power and efficiency. Energy Convers Manag 2021;11. [Crossref]
[24] Li D, King M, Dooner M, Guo S, Wang J. Study on the cleaning and cooling of solar photovoltaic panels using compressed airflow. Sol Energy 2021;221:433–444. [Crossref]
[25] Almuwailhi A, Zeitoun O. Investigating the cooling of solar photovoltaic modules under the conditions of Riyadh. J King Saud Univ Eng Sci 2023;35:123–136. [Crossref]
[26] Abdullah AA, Attulla FS,. Ahmed OK, Algburi S. Effect of cooling method on the performance of PV/Trombe wall: Experimental assessment. Therm Sci Eng Prog 2021;30: 101273. [Crossref]
[27] Abdullah AA. The effect of operating conditions and climate change on the performance of the photopholtaic Trombe wall: An empirical estimate. J Therm Eng 2024;10:1241–1252. [Crossref]
[28] Rathore A. Energy, exergy and performance analysis of a 380 kWP roof-top PV plant assisted with data-driven models for energy generation. J Therm Eng 2024;10:1164–1183. [Crossref]
[29] Hamzawy AH, Abed QA, "An experimental study on the impact of porous media in improving the heat transfer performance characteristics of photovoltaic-thermal system. J Therm Eng 2025;11:181–195. [Crossref]
[30] Wang G, Yang Y, Yu W, Wang T, Zhu T. Performance of an air-cooled photovoltaic/thermal system using micro heat pipe array. Appl Therm Eng 2022;217:119184. [Crossref]
[31] Nabil T, Mansour TM.Augmenting the performance of photovoltaic panel by decreasing its temperature using various cooling techniques. Results Eng 2022;15:100564 [Crossref]
[32] Tian MW, Khetib Y, Yan SR, Rawa M. Energy, exergy and economics study of a solar/thermal panel cooled by nanofluid. Case Stud Therm Eng 2021;28:101481. [Crossref]
[33] Mazón-Hernández R, García-Cascales JR, Vera-García F, Káiser AS, Zamora B. Improving the electrical parameters of a photovoltaic panel by means of an induced or forced air stream. Int J Photoenergy 2013;2013. [Crossref]
[34] Hernandez-Perez JG, Carrillo JG, Bassam A, Flota-Banuelos M, Patino-Lopez LD. A new passive PV heatsink design to reduce efficiency losses: A computational and experimental evaluation. Renew Energy 2020;147:1209–1220. [Crossref]
[35] Feng S, Shi M, Yan H. Sun S, Li F, Lu TJ. Natural convection in a cross-fin heat sink. Appl Therm Eng 2018; 132; 30–37. [Crossref]
[36] Huang GJ, Wong SC, Lin CP. Enhancement of natural convection heat transfer from horizontal rectangular fin arrays with perforations in fin base. Int J Therm Sci 2014;84:164–174. [Crossref]

[37] Shaeri MR, Bonner R.Laminar forced convection heat transfer from laterally perforated-finned heat sinks. Appl Therm Eng 2017;116:406–418. [Crossref]
[38] Chu WX, Lin YC, Chen CY, Wang CC. Experimental and numerical study on the performance of passive heat sink having alternating layout. Int J Heat Mass Transf 2019;135:822–836. [Crossref]
[39] Kanargi B, Lee PS, Yap C.International Journal of Heat and Mass Transfer A numerical and experimental investigation of heat transfer and fluid flow characteristics of an air-cooled oblique-finned heat sink. 2018;116:393–416. [Crossref]
[40] Çengel YA, Ghajar AJ, Kanoğlu M.Heat and mass transfer : fundamentals & applications.
[41] Hadipour A, Rajabi Zargarabadi M, Rashidi S. An efficient pulsed- spray water cooling system for photovoltaic panels: Experimental study and cost analysis *Renew Energy* 2021;164:867–875. [Crossref]
[42] Peng Z, Herfatmanesh MR, Liu Y. Cooled solar PV panels for output energy efficiency optimisation. Energy Convers Manag 2017;150: 949–955. [Crossref]
[43] Subasi A, Sahin B, Kaymaz I. Multi-objective optimization of a honeycomb heat sink using Response Surface Method. Int J Heat Mass Transf 2016;101:295–302. [Crossref]
[44] Singh V, Yadav VS. Optimizing the performance of solar panel cooling apparatus by application of response surface methodology. 2022;236. [Crossref]
[45] Singh V, Yadav VS. Application of RSM to Optimize Solar Pump LCOE and Power Output. 2022;69:1–12. [Crossref]
[46] Singh V, Yadav VS, Saxena V, Kumar N, Maheswari A. Theoretical Analysis of 1st Law and 2nd Law Efficiency of a Solar Pump for Geographical Location 28.10'N, 78.23'E. Lect Notes Mech Eng 2022;411–417. [Crossref]
[47] Waila VC, Sharma A, Singh V, Gupta NK. Solar photovoltaic water pump performance optimization by using response surface methodology. Environ Prog Sustain Energy 2023. [Crossref]
[48] Choudhary S, Sharma A, Gupta S, Purohit H, Sachan S. Use of RSM technology for the optimization of received signal strength for LTE signals under the influence of varying atmospheric conditions. Evergr Jt J Nov Carbon Resour Sci Green Asia Strateg 2020;07:500–509. [Crossref]
[49] LMA Campos, Moura HOMA, Cruz AJG, Assumpção SMN, de Carvalho LS, Pontes LAM. Response surface methodology (RSM) for assessing the effects of pretreatment, feedstock, and enzyme complex association on cellulose hydrolysis. Biomass Convers Biorefinery 2020:12;1–12. [Crossref]
[50] Response Surface Methodology (RSM) flowchart. https://www.researchgate.net/figure/Response-Surface-Methodology-RSM-flowchart_fig1_316577916 Accessed on Sep 27, 2022.
[51] Le HS, Galal A, Alhamrouni I, Aly AA. Heat transfer efficiency optimization of a multi-nozzle micro-channel heat sink utilizing response surface methodology. Case Stud Therm Eng 2022;37:102266. [Crossref]
[52] Chiang KT, Chang FP. Application of response surface methodology in the parametric optimization of a pin-fin type heat sink. Int Commun Heat Mass Transf 2006;33:836–845. [Crossref]
[53] Onokwai AO, Owamah HI, Ibiwoye MO, Ayuba GC, Olayemi OA. Application of Response Surface Methodology (RSM) for the optimization of energy generation from Jebba hydro-power plant, Nigeria. ISH (J Hydraul Eng) 2020;28:1–9.
[54] Qader BS, Supeni EE, Ariffin MKA, Talib ARA. RSM approach for modeling and optimization of designing parameters for inclined fins of solar air heater. Renew Energy 2019; 136:48–68. [Crossref]
[55] Rout A, Singh S, Mohapatra T, Sahoo SS, Solanki CS. Energy, exergy, and economic analysis of an off-grid solar polygeneration system. Energy Convers Manag 2021;238:114177. [Crossref]
[56] Karami N, Rahimi M. Heat transfer enhancement in a PV cell using Boehmite nanofluid. 2014;86:275–285. [Crossref]
[57] Trivedi V, Saxena A, Javed M, Kumar P, Singh V. Design of Six Seater Electrical Vehicle (Golf Cart). Evergreen 2023;10:953–961. [Crossref]
[58] Chandel SS, Agarwal T. Review of cooling techniques using phase change materials for enhancing efficiency of photovoltaic power systems. Renew Sustain Energy Rev 2017;73:1342–1351. [Crossref]
[59] Kumar M, Ansari NA, Sharma A, Singh VK, Gautam R, Singh Y. Prediction of an optimum engine response based on various input parameters on common rail direct injection diesel engine-a response surface methodology. Available at: https://scholar.archive.org/work/7wxig7vx2naklk3futcbp36jmi/access/wayback/http://scientiairanica.sharif.edu/article_22272_8d700f88d1a63567d2e8ea087bbbacb0.pdf. Accessed: Jul. 30, 2022.
[60] Singh V, Trivedi V, Mishra VR. Use of response surface methodology and CFD for analysing and optimization of simple-air cooled solar panel. Int J Energy Water Resour 2024:0123456789. [Crossref]
[61] Shrivastava A, Jose JP, Borole YD, Saravanakumar R, Sharifpur M, Harasi H, et al. A study on the effects of forced air-cooling enhancements on a 150 W solar photovoltaic thermal collector for green cities. Sust Ener Tech Assessments 2022;49:101782. [Crossref]
[62] Sainthiya H, Beniwal NS. Comparative analysis of electrical performance parameters under combined water cooling technique of photovoltaic module: An experimental investigation," Energy Sources Part A Recover. Util Environ Eff 2020:42:1902–1913. [Crossref]
[63] Ali AA, Lafta DA, Noori SW, Abdulamir F, Rashid FL. Innovative materials integrated with PCM for enhancing photovoltaic panel efficiency: An experimental investigation. J Energy Storage 2024:102. [Crossref]

APPENDIX

Calculation of cell Temperature

The cell temperature was calculated using the energy balance of the solar panel and the Nominal Operating Cell Temperature (NOCT) conditions.

$$T_{Cell} = \frac{T_a + (T_{CNOCT} - T_{aNOCT})\left(\frac{G_T}{G_{TNOCT}}\right)\left(1 - \left(\frac{\eta_{mpSTC}(1 - \alpha_p T_{cSTC})}{\tau\alpha}\right)\right)}{1 + (T_{CNOCT} - T_{aNOCT})\left(\frac{G_T}{G_{TNOCT}}\right)\left(\frac{\alpha_p \eta_{mpSTC}}{\tau\alpha}\right)}$$

From the solar panel manufacturer data

$$T_{CNOCT} = 48°C, T_{aNOCT} = 20°C, G_{TNOCT} = 800\frac{W}{m^2}, \qquad T_{CSTC} = 25°C, \eta_{mp} = 0.154,$$
$$\tau\alpha = 0.9, \alpha_p = -\frac{0.002726}{°C}$$

Put these values in the above equation, the cell temperature equation in terms of the atmospheric temperature and the solar flux.

$$T_{Cell} = \frac{T_a + 0.022946 G_T}{1 - 0.0000181279 G_T}$$

So when Ta = 45°C and G_T = 1000 W/m^2

T_{Cell} = 69.20°C

The top surface heat transfer coefficient at airflow velocity of V = 3 m/s

$$h_T = 2.8 + 3V = 2.8 + 3 * 3 = 11.8\, W/m^2 k$$

The radiation heat transfer coefficient

$$h_r = \varepsilon\sigma(T_C + T_a)(T_C^2 + T_a^2)$$
$$\varepsilon = 0.83, T_C = T_{average} = 57.21°C, T_a = 45°C$$
$$h_r = 6.41\, W/m^2 k$$

So total heat transfer coefficient from the top surface of the solar panel

$$h_e = h_c + h_r = 11.8 + 6.41 = 18.21\, W/m^2.k$$

Total heat transfer

$$Q_{Top} = (T_{Cell} - T_a)/(\frac{L_{EVA}}{K_{EVA}} + \frac{L_{ETFE}}{K_{ETFE}} + \frac{1}{h_e})$$

L_{EVA}= 0.20 mm, K_{EVA}=0.35 W/mk, LETFE= 0.28 mm, K_{ETFE} = 0.24 W/mk

$$Q_{Top} = 427.1965\frac{W}{m^2}$$

Now EVA plate temperature

$$T_{EVA} = T_{Cell} - \left(\frac{L_{EVA}}{K_{EVA}}\right) Q = 68.12°C$$

Now ETFE plate temperature

$$T_{ETFE} = T_{EVA} - \left(\frac{L_{ETFE}}{K_{ETFE}}\right) Q = 67.4°C$$

Now efficiency of solar panel

$$\eta = \eta_{mp}(1 + \alpha_{STC}(T_C - T_{CSTC})$$

$$\eta = 0.154(1 - 0.002726(69.42 - 25) = 0.1353$$

Percentage reduction in solar panel efficiency

$$\%\Delta\eta = \frac{0.154 - 0.1353}{0.154} = 12.28\%$$

The power output from solar panel

$$P = P_m(1 - \alpha_P(T_{cell} - T_{CSTC}) = 10(1 - 0.002726(69.42 - 25) = 8.78\ W$$

Bottom layer of solar panel temperature

Heat transfer from bottom of solar panel

$$\mathrm{Q_{Bottom}} = \mathrm{A_P} * \mathrm{I_t} * \alpha - \mathrm{P} - \mathrm{Q_{Top}}$$

$$\mathrm{Q_{Bottom}} = 0.071 * 1000 * 0.97 - 8.78 - 427.19 * 0.071$$

$$\mathrm{Q_{bottom}} = 29.75\ \mathrm{W} = \frac{29.75}{0.071} = 419.14\frac{\mathrm{W}}{\mathrm{m^2}}$$

Temperature of bottom layer

$$\mathrm{T_{Bottom}} = \mathrm{T_{cell}} - \left(\frac{\mathrm{L_{EVA}}}{\mathrm{K_{EVA}}} + \frac{\mathrm{L_{PET}}}{\mathrm{K_{PET}}} + \frac{\mathrm{L_{CFRP}}}{\mathrm{K_{CFRP}}} + \frac{\mathrm{L_{Tape}}}{\mathrm{K_{Tape}}}\right) * \mathrm{Q_{Bottom}}$$

$$T_{Bottom} = 68.24°C$$

Exergy Analysis

Exergy reached on the surface of solar panel

$$E_{SUN} = A_P I_t[1 - \tfrac{4}{3}\left(\tfrac{T_a}{T_{SUN}}\right) + \tfrac{1}{3}\left(\tfrac{T_a}{T_{SUN}}\right)^4]$$

Put I_t =1000 W/m^2, Ta = 318 K, T_{Sun} =5770 K, Ap =0.071 m^2

$$E_{SUN} = 64.85\ W$$

Exergy efficiency

$$\varphi = \frac{W_e}{E_{SUN}}$$

$$\varphi = 13.44\ \%$$

Uncertainty Calculations

Uncertainty in the power output of solar panel

The power of the solar panel›s maximum voltage and current

$$P = f(I, V)$$

So uncertainty in the power production of solar panel

$$y_P = \sqrt{\left(\frac{\partial P}{\partial I}\right)^2 y_I^2 + \left(\frac{\partial P}{\partial V}\right)^2 y_V^2}$$

The uncertainty in the current $y_I = 3\%\ and\ in\ Voltage\ y_V = 3.5\%$. The measurement of the current at some time is the 0.8 amp and V = 10 V.

Now uncertainty in the current $y_I = 0.8 * \frac{3}{100} = 0.024$

Uncertainty in the voltage $y_V = 10 * \frac{3.5}{100} = 0.35$

$$P = VI \quad so\ that \frac{\partial p}{\partial I} = V\ and \frac{\partial P}{\partial V} = I$$

So uncertainty in power measurement

$$y_P = \sqrt{(V)^2 y_I^2 + (I)^2 y_V^2}$$

$$y_P = \sqrt{(10)^2 (0.35)^2 + (0.8)^2 (0.024)^2}$$

$$y_P = 3.5\%$$